

TECHNICAL REPORT

A 3D model for kinematic analysis of equine locomotion

Methodology for a 3D biomechanical model of the horse

**) Framework of Equine Biomechanics models and scoping of this Report*

**) Morphological segments structure and mechanical segments applied to equine's morphology and the rigid bodies of the biomechanical model*

**) Markers set and 3D segments orientation for data collection*

**) Joints angular references based on the relative 3D orientation and model's vectors define by placement of markers.*

**) Example of 3D kinematic data vs. time of a set of trials*



PTDC/CVT-CVT/32613/2017: EquiPerfoRM

Three-dimensional motion analysis for monitoring of rehabilitation and high-performance training of the equine athlete.

supported by:

FCT
Fundação para a Ciência e a Tecnologia
MINISTÉRIO DA EDUCAÇÃO E CIÊNCIA
September, 2022

A 3D model for kinematic analysis of equine locomotion

Methodology for a 3D biomechanical model of the horse

Index

1. Framework of Equine Biomechanics models	4
2. Scoping of this Report and survey of work with motion capture systems.....	8
3. Morphological segments structure and mechanical segments.....	11
3.1. Head, Neck and Trunk.	11
3.2. Forelimb	12
3.3. Hindlimbs.....	15
4. The equine’s morphology and the rigid bodies of the biomechanical model.....	16
4.1. The skeleton and the placement of the reflective markers	18
4.2 Definition of 3D mechanical segments orientation for data collection	19
5. Markers set and 3D segments orientation for data collection.....	19
5.1 Segment: Head	20
5.2 Segment: Neck	20
5.3 Segment: Trunk (Body) and the three parts: thorax, back spine, and tail	21
5.4 Segment: Scapula	23
5.5 Segment: Humerus.....	24
5.6 Segment: Radius and Ulna	25
5.7 Segment: Metacarpus	25
5.8 Segment: Fore Pastern (P1+P2).....	26
5.9 Segment: Fore Hoof	27
5.10 Segment: Pelvis	27
5.11 Segment: Femur	28
5.12 Segment: Tibia and Fibula	28
5.13 Segment: Metatarsus	29
5.14 Segment: Hind Pastern (P1+P2)	31
5.15 Segment: Hind Hoof (left; right).....	31
6. Joints angular references based on the relative 3D orientation	33
7. Model’s vectors. Placement of markers. Joints movement patterns	36
Joint #1	36
Joint #2	37
Joint #3	39
Joint #4	41
Joint #5	42

Joint #6	44
Joint #7	45
Joint #8	47
Joint #10	50
8.Example of 3D kinematic data vs. time of a set of trials	51
8.1. The pace	51
8.2. The angular kinematic pattern	52
BIBLIOGRAPHY OF REFERENCE.....	55

My epistemological thinking about the Biomechanics of Movement always has two initial assumptions

“LIFE does not create Laws of Physics, it adapts to them”

“We don't think in muscles, we think in movements and supports.”

1. Framework of Equine Biomechanics models

From the available methods, there is an evolution of laboratory assessments for analysis of equine locomotion, monitoring and diagnosis of the activities that result in better welfare, training or treatment of those involved. The crucial point common point to all methods of locomotion analysis is the preservation of the horses' health by making these methods as non-intrusive as possible and contributing to the horses' overall health. General examples of analysis application are, the monitoring the effect of work with young animals, contributions to the understanding of the evolution or loss of performance, monitoring of sport training programs, or more specifically, the evaluation of lameness and the monitoring of its recovery.

Adapted from previous texts about conceptual positioning of Biomechanics of Motion as an interdisciplinary scientific area (Abrantes, 2019)¹ I quote that a parallel framework can be established between the fundamentals of biomechanical studies of motion and the characteristics of self-control systems.

In biomechanical studies, the multiplicity of motor responses given by the horse, through its locomotor system, is related to the influence and integration of intrinsic factors of this system. Namely, integrating and comparing to the extent possible: the architecture of an artificial self-control system with characteristics studied by the morphology of the horse; the process of system control compared with the horse's neurological influences, giving the ability to control the relationship with the external environment; or, the process of energy flows of the system with the physiological homeostasis in the horse.

When compared to the influence of the interaction of those factors - which constitute the general background of motor performance - the scope of movement analysis of horse locomotion is partial and limited. However, in on the other hand, we can note that it is the

¹ Abrantes, João (2019) Fundamentos e Elementos de Análise em Biomecânica do Movimento Humano. Edição MovLab:<https://movlab.ulusofona.pt/wp-content/uploads/sites/202/2020/11/Fundamentos-e-Elementos-de-analise-edicao-2019.pdf>

visible aspects of the horse's performance, observed and recorded, that are the first source of data to find the first supporting explanations of motor behaviour.

Therefore, the function of relating to the external environment is achieved, essentially, by the externalisation of the mechanical function of a system - the biomechanical system - which is integrated in a more general system that is self-controlled. Consequently, the self-controlled motor production is the mechanical consequence, or product, of the operational and control process of the biomechanical system. Product that is an integral part of the general behaviour of the biological system and in particular a consequence of the processes proper to the horse under observation: whether in visible aspects or in deduced aspects; whether in the body of that performer or in the effects caused outside.

The object of study of the Biomechanics of motor behaviour is thus defined as the non-deterministic, therefore, standardised but not robotic, production of the locomotor system resulting from external mechanical solicitations and the biological responses organised into displacements according to the purpose of the motion. These responses are products of the biomechanical system. The biomechanical analysis and associated methods collect data from the visible products that are accessible through the displacements, i.e., the kinematics of the performance, while the non-visible products are accessible through the force effects, the dynamics of the performance.

It is evident that an experienced equine behaviourist has the knowledge and experience to visually assess each horse providing the basis for training or clinical interventions. However, the objectification of horse movement examinations based on data resulting from laboratory analyses constitute a database, firstly for future memory and detailed monitoring, or to constitute knowledge bases in veterinary or other teaching, constituting the foundations of an evidence based practice of future stakeholders as they can then review, analyse and, ideally, translate the latest scientific evidence in the area of equine movement analysis.

The registration of horse's movement has historical relevance for the scientific area of biomechanics in general and in its specificities when analysing movements of humans or animals. In fact it was the technological development work of Eadweard J. Muybridge (1830-1904) that contributed to the recording by images of movement. Thus began the phase of moving from visual observation, without objective data, to technology-based objectification based on the use of images. And horses were its first examples of application.

Muybridge based his technology on the use of sequentially acting photographic cameras with regular time intervals (24 images per second), placed in parallel but positioned so as to capture, at different distances, sequential images of a horse's locomotion (Muybridge, 1878) but in such a way that the horse was framed by spatial references placed in the cameras' field of

view, but the horse must have the displacements parallel to the space references. The book in reference has about seven dozen examples of different forms of locomotion with the horse led by the rider and just one the horse is free of rider. In each sequence for the same performance, the set of images have a defined temporal interval and, in common, spatial references localized on the path of locomotion evolution.

The aim of the present review is to be concentrate in the assessment of the horse's kinematics not about the historical development of biomechanical methods applied to horses since sec XIX. However, Muybridge in an apparently independent way of the methodology used to study the displacements, at the end of the mentioned book, presents ten photos of the horse's skeleton in different positions. Again, it is possible to refer Muybridge as the precursor of one of the essential points for the first stages of the elaboration of a biomechanical model: the definition of the anatomical segments defined as the basis of a biomechanical model.

In parallel, Wilhelm Braune and Otto Fischer (1889) developed the first works of three-dimensional analysis applied to human locomotion. Despite the methodological limitations, the authors developed important points for the analysis of movement, such as the location of body's centre of gravity and the intersegmental rotation centres.

The methodologies described already contains the essential elements of current methodologies for capturing images for analysis: high-frequency recording and spatial references common to all the images. Or, simply, to study the horse's kinematics characteristics.

Nowadays, for study the horse's kinematics, images are collected at least at 100 frames per second for each one of the set of cameras (10 or more it depends of the laboratory budget) and the three-dimensional spatial location is related in two ways: first, all markers or other defined anatomical points are related to an origin of the volume of evolution of the locomotion. This origin is the zero point of all linear measurements; second, a set of three dimensional axis fixed to each mechanical segment. Each axis define the relative position in relation to the correspondent axis of the adjacent segment. The dot product of the correspondent axis of reference compute the relative rotational measurements in each plane.

The association of the horse skeleton and the methodology of finding the body segments centre of intersegmental rotation, gives the background of the transition from anatomical segments to mechanical segments of the biomechanical model. Very briefly, the definition today of the number of segments of the model is dependent on the number and definition of the anatomical segments into which the horse is "divided". For each anatomical segment, the locations of the markers (passive reflectors for the infrared light emitted by the cameras) are studied, which make it possible to have three-dimensional spatial references for the respective

mechanical segments of the model and their coherent spatial relationship. Spatial definition that relates the 3D orientation of each segment coherently with the adjacent segments in order to define the potential intersegmental three-dimensional rotations.

The development of a biomechanical model comprises not only the equipment described above, in a very small way, but also a set of logistical aspects inherent to the complexity of the elaboration of the biomechanical model. A horse biomechanical model can only be developed with the integrated work of a set of specialists, necessarily, on Veterinary, on Biomechanics, and on Computer science. A serious issue is the adequate laboratory space, both in dimensions and lighting characteristics (3D image acquisition systems do not work in places with daylight falling on the aforementioned space). The availability of a specific horse and its handling during data acquisition is another issue to consider. Also important to consider the computer processing and interpretation of each horse's data because it is very time consuming, even if done in an integrated process by the set of specialists cited above.

Interpretation of the data can be studied by a brief definition encompassing two concepts of the horse locomotion. The first is related with the pace during the forward progression. The pattern of the pace for walk, trot and gallop have different organizations and the interpretation work with the variability of the spatiotemporal parameters such as stride length, if possible divided on support phase and swing phase, cadence and locomotion speed.

The second concept is related with the pattern of the limbs motion that organize the manner of inter segmental angular progression in accordance with the pace in the support phase and on the swing phase of each single limb and the correspondent temporal synchronization with the other ones. A basic biomechanical concept demonstrates that the mechanical energy flows from the "fixed" mechanical segment to the "free" one. In support phase the mechanical energy flows from the upper segment to the support segment, in the swing phase it happens the opposite. The cited mechanical energy depends from morphological components combine with the intersegmental angular velocity. The morphological (segment length and inertia) do not change but the self-control angular velocity will be determinant to understand the flow and quantification of mechanical energy.

In both concepts the variability is present from stride to stride as result of a normal motor behaviour defined as non-deterministic, therefore, standardised but not robotic. For the first concept the pace during the forward progression is studied by descriptive statistics. For the second one, the adequate and more simplified solution is to study the behaviour variability, first isolating each stride from a homogeneous set of the same locomotion type (walk, trot, etc.) and form a wave that represents one stride behaviour; second checking the coefficient of variation of the set

of waves found. The proposed process is the application of the wave-coefficient of variation (Winter, 2009)².

2. Scoping of this Report and survey of work with motion capture systems

In two dimensional (2D) studies of equine walking, angular variables are generally treated as flexion and extension in the sagittal plane. Since the joints of the equine's limbs evolved to move primarily under the sagittal plane, most studies and kinematic variables can be captured laterally to the equine, under a 2D plane. In addition to the 2D analysis, a 3D model is required for a more detailed specific analysis. This technical report aims to characterize an equine 3D model. The purpose is to report the methodology followed based on the anatomical and biomechanical criteria, using a Vicon system and complementary software for data reduction. However, for studies carried out in the field of sport or in diagnosis and rehabilitation, it is important to study adduction / abduction and/or internal / external rotations, which is only possible with three-dimensional (3D) analysis.

This report is related with the use of a Vicon system and complementary software for data reduction, i.e., a system of motion capture that works with passive reflective markers and the full body reconstruction support by Nexus software based on the criteria described below. In brief, Vicon (hardware) + Nexus (software) work integrated to support the reconstruction of the model. However, Nexus is "blind" about new models. In the case of full body horse models it was necessary to start from scratch and define all steps. There are not a commercial or free model set for use in horses. We intend to fix the "HorseModel" and offer to the community of Equine Biomechanics in an open access basis.

In the present case the project developed all steps. Very briefly, after each session of data capture (a single day of work) is necessary the "secretary" work of reconstruct the data, from recognize more than hundred passive markers glued in the horse in the same order defined previously in the theoretical model, recognize their location (one by one for each trial) in the 3D image and reconstruct a C3D file, define (by visual definition) the limits of support phase and swing phase of each step, etc. until the trial graphics output. The details of the model formulation - before field work could be done - are described in the next few pages.

² Winter, D. (2009). *Biomechanics and Motor Control of Human Movement*(4th ed.). Hoboken, New Jersey: John Wiley & Sons, Inc.

A simple survey on similar systems with which kinematic data of the horse's locomotion was obtained - of the last three decades - demonstrate a vast amount of interesting studies. The literature search was based essentially on the databases: PubMed, ScienceDirect. All of them demonstrated that is necessary a team of specialists that make an integration effort to achieve results and studies that, potentially, give signals, suggestions, to future directions.

HARDWARE and SOFTWARE: The first observation is about the type of hardware and software ("systems") used for motion capture. The "Qualisys" system (originally from Sweden) is, for the last twenty years, the most widely used (around 57% worldwide). This system is used mainly outside the United States where the "Motion Analysis Corporation" system is predominantly used. The "Vicon" system (used in the current project) has little representation. Understandable options. "Qualisys" is cheaper than systems in the same range and provides fixed software for horse motion analysis. The diffusion of the American system "Motion Analysis Corporation" may be due to the fact that it is the preferred system of Professor Hilary Clayton³. The improvement of the Vicon system was chosen by the project because it is a continuity of the same hardware already existing in the MovLab. "Vicon" has a very reliable hardware (preferred big movie companies) and a software (the Nexus) that is very "open" enabling the development, from scratch, of new biomechanical models. Other systems are very poorly represented and are mostly a local adaptation of a set of video cameras with associated appropriate software. What is very common is that authors indicate that they use locally developed software for data processing. But one constant is that it is not explained (with a minimum of detail) the details of the methodologies used, namely, what processes and what they are based on are used to draw the kinematic behaviour curves. We also find no methods for calculating the average curve of all the curves and their coefficient of variation.

In this particular, the current project has already developed software based on David Winter's Waves Coefficient of Variation as mentioned in the end of point 1.

The methodologies of the studies are described within what is necessary but not enough for anyone wishing to replicate and design the same biomechanical models used. The kinematic evaluation of the horses is performed in a specific way for the variables presented. The aim of the current project is to construct and disseminate a model as a tool of analysis, freeware, first for the colleagues with Vicon systems but also free to anyone want to develop the same model.

³ Professor Hilary Clayton is consultant of the current project and co-author of articles with our Laboratory. She is a McPhail Dressage Chair Emerita, Michigan State University

Methodologies that perform a whole-body model are rare. Generally the methodologies do not apply many reflective markers and therefore do not spend much time on data acquisition and processing. Consequently, papers presents data results for few variables. The most common are about spatiotemporal data and the flexion-extension component of some of the angles of the hindlimbs and forelimbs. The projects work, preferably, with healthy horses.

INJURIES: Studies in horses with injuries are very few. I have not found any paper that monitored medical treatments, as the project intended to do. But of those read, one article studied the effect of Kinesiotape, that theoretically stimulates mechanoreceptive.

However the lameness is considered. Lameness is a significant problem in the equine health. It is considered the number one cause of handicap performance in horses of all ages and all breeds. In the examples listed it is the most represented disease. Lameness was the underlying topic of the studies present in the two master's theses completed in the first year of the project. Unfortunately, for reasons presented in previous reports the application of the developed model was not developed. In this particular topic I highlight 5 leading authors:

Keegan, K. (1998) lead a working group involving interns in veterinary medicine do the evaluation of mild lameness related with assessments with kinematic gait. The same Keegan (2007) in a review about the subject wrote about an important issue: *“Kinematic and kinetic gait analysis potentially offers veterinarians an objective method of determining equine limb lameness. Subjective analyses have been shown to be somewhat flawed, and there does not seem to be a high degree of intraobserver agreement when evaluating individual horses.”*.

Fuller et al. (2006) studied the influence of anaesthesia on assessing after local anaesthetic. Bragança, F., et al. (2021), the horses with lameness strategies (walking on treadmill); Alvarez, G. (2007), the effect of induced limb lameness on thoracolumbar kinematics, walking on treadmill; Hewetson, et.al. (2006), the reliability of observational gait analysis for the assessment of lameness.

SAMPLE SIZE: The number of horses is a main issue in equine kinematic studies describe in Bystrom et al (2018), Seino et al. (2019) and Gmel et al. (2022) as a limitation. In Ericson et al. (2020) explain that with a low number of horses used the conclusions of the results are restrict. The issue even bigger when we have a small population with horses from different disciplines, ages, and levels (Hardeman et al. 2020; Hardeman et al, 2019).

However most of the papers consulted have a very small sample size. Without wanting to generalize for all the studies already done around the world, we found more than 50% of the samples below 10 horses, or 80% below 25 horses.

Some exceptions stand out in the “bibliography of reference”: Roepstorff et al (2021) with 222 horses (the the walking rhythm of the horses was obtained with a force plate and with a couple of markers the vertical tilting of the pelvis). Kallerud et al. (2021) - 103 horses (A few markers to study the symmetry parameters based on the difference between head minimum and maximum positions and the difference between pelvis minimum and maximum positions.). Hardeman et al. (2022) -122 horses (Study of kinematic parameters of spatiotemporal variables: speed, vertical range of motion of the head, withers, and pelvis). Rhodin et al.(2022) – 65 horses (The study of kinematic data was study based on inertial sensors, not in markers attached to the horse).

Although the horse's whole body model is valuable for studying the effects of interarticular (or intersegmental) coupling, the examples pointed out as "exceptions" may constitute a methodological path that: first, is much less time consuming in data acquisition and processing for each horse; second, responds much faster and more reliably to the questions posed by veterinarians; third, provides clues for the application of more complex methodologies, such as the application of whole body models; fourth, makes biomechanical assessment cheaper.

3. Morphological segments structure and mechanical segments

3.1. *Head, Neck and Trunk.*

The head of the horse is composed of 16 bones and these are classified according to their location, being the bones of the neurocranium (brain box): Occipital, Sphenoid, Ethmoid, Interparietal, Parietal, Frontal and Temporal; and viscerocranial bones (face): Maxillary, Nasal, Lacrimal, Zygomatic, Incisor, Vomer, Palatine, Pterygoids and Mandible.

The spine starts from the skull and goes to the tip of the tail. It consists of bones called vertebrae. The sequence from the skull is as follows: Atlas, Axis, cervical vertebrae, thoracic vertebrae, lumbar vertebrae, sacral vertebrae and caudal or coccygeal vertebrae. The functions of the spine are the protection of the spinal cord, movements of flexion, extension, and rotation, in addition to supporting the body and various organs such as stomach and intestines.

The ribs are elongated and curved; its body is more rounded than flat. The extremities are articulated to the thoracic vertebrae and the sternum. They have the function of protecting organs such as heart and lungs and assist in the breathing process, together with the diaphragm.

The sternum is formed by three parts: manubrium cartilage, sternum body (sternum) and xiphoid cartilage. They assist in the protection and support of organs. It articulates laterally with the ribs on the right and left side, forming the rib cage.

Figure 1 shows the anatomical marks of the head, neck and trunk axes and their reflective markers proposed in the construction of the three-dimensional biomechanical model presented in this technical note. The markers on the right and left side are fixed in a similar way (with some symmetry).

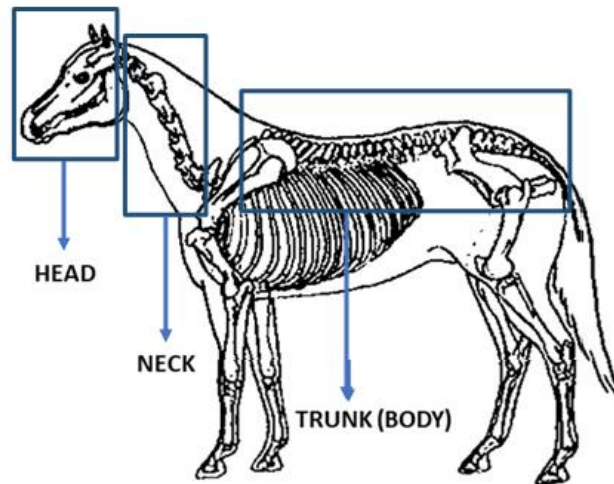


Figure 1: Head, Neck and Trunk segments in the Equine Three-dimensional Biomechanics Model. Source: *EquiPERFORM project data*, 2022.

3.2. Forelimb

The forelimb is formed by the bones: scapula, humerus, radius and ulna (forearm), carpal bones, 3rd metacarpus, 2nd and 4th metacarpus, proximal sesamoids, 1st phalanx (proximal), 2nd phalanx (middle), 3rd phalanx (distal) and distal sesamoid (navicular bone).

The Scapula Bone is shaped like a tennis racket, being mostly a flat bone. It is linked to walking, being responsible for stretching the thoracic limbs (bringing the arm back and forth in the walking process). That is why the angle of the Scapula is important for the morphological evaluation of horses, since, from it, we can know if the animal's step is long or not, being important for running animals (the more horizontal the angle, the better, because the longer is the animal's step, the greater the stretch of the arm).

It is positioned on the ribs connected by muscles and tendons and is articulated to the humerus. The equine humerus has the intermediate tubercle as a feature, in the lateral direction. It is a long bone; it is articulated to the Scapula and to the bones Radio and Ulna.

Radio and Ulna are fused together, and Ulna extends throughout the entire body of the Radio (unlike ruminants where Ulna ends up in the middle of the Radio's body). They are long

bones and articulate with the Humerus and the Carpus. They perform the movement of raising and lowering the arm.

Carpal bones are irregular and small. They are arranged in accessory carpal (lateral face), ulnar carpal (lateral face), intermediate carpal, O. radial carpal (medial face), carpal II and carpal III (which are fused) and carpal IV (lateral). These bones form the knee region in horses. They are linked to Radio and Ulna, and Metacarpus.

The metacarpus is a long bone. Arranged in metacarpal IV, metacarpal III (the longest of all metacarpal bones, it is between the other two) and metacarpal II. Bones IV and II are fused in III, and their length extends to the middle of the body of the metacarpal III. They are articulated with the carpal bones, the proximal sesamoid, and the proximal phalanx.

Sesamoids are irregular and square. The proximal sesamoid has a protective function of the metacarpals when walking, if the impact is large and they touch the floor. And the distal sesamoid (navicular bone) has a protective function of the hull in the impact of walking.

The articulation between the metacarpal bones, proximal sesamoids and proximal phalanx forms the anatomical region called fetlock. A region that suffers a lot from the exaggeration of physical activity, getting the ligaments compromised, causing swelling and a lot of pain to the animals.

The phalanges are divided into proximal, middle, and distal (surrounded by the hull). The proximal is articulated to the metacarpal and sesamoid, and the distal phalanx is articulated to the distal sesamoid. The phalanges that remained in the equine species were only the III (third finger, the other phalanges have evolved over the course of evolution). They are considered long bones.

Due to their proximity to the center of gravity, the forelimbs mainly have a supporting role, supporting about 58% of the weight^{2; 14;15}.

Horses do not have a collarbone, the forelimb being connected to the trunk only through muscles (sinsarcosis), which allows greater scapular mobility and, consequently, an increase in stride length. These muscles are called extrinsic, with insertions in the limb and trunk¹⁶. Intrinsic muscles are the muscles of the limb itself. The intrinsic ones are smaller in volume, when compared to the extrinsic musculature, with short and strained muscle fibers as well as long tendons¹⁷.

The thoracic limb of horses shows concentrated muscle groups proximally, which extend over long tendons as they move towards distal, allowing the creation of a passive system of "springs" and thus reducing the cost of locomotion^{17;18;19}.

The tendons of vertebrate animals have a uniform constitution and low energy dissipation. When tension is exerted on these tendons, they return about 93% of elastic energy, with only 7% being dissipated in the form of heat^{20,17}.

Figures 2 and 3 show the anatomical marks of the segments scapula, humerus, radius and ulna (Forearm), fore fetlock, pastern (Fore P1+P2) and fore hoof and their respective reflective markers (44 marks) proposed in the construction of the biomechanical model three-dimensional model proposed in this technical note. The markers were placed on the forelimbs on the left right side of the horse.

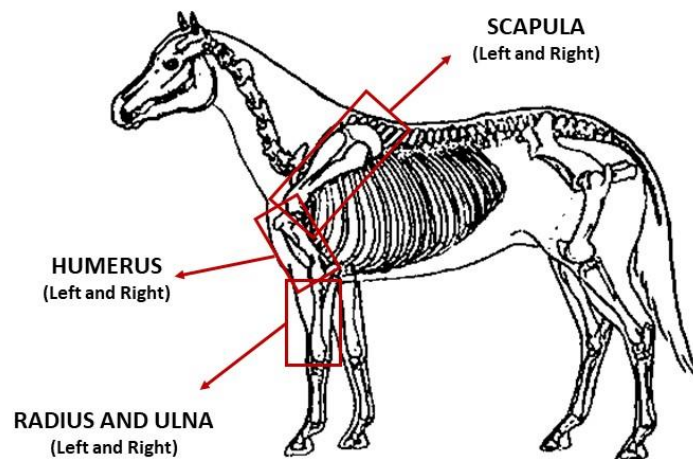


Figure 2: Forelimb upper segments: Scapula, Humerus, Radius and Ulna in the Equine Three-dimensional Biomechanics Model. Source: *EquiPERFORM project data*, 2022.

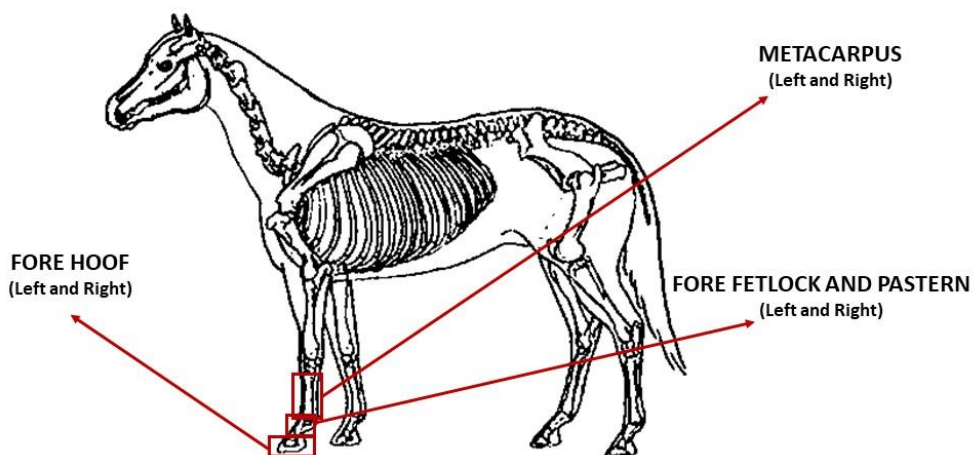


Figure 3: Forelimb lower segments: Metacarpus, Fore Pastern (Fore P1+P2) and Fore Hoof in the Equine Three-dimensional Biomechanics Model. Source: *EquiPERFORM project data*, 2022.

3.3. Hindlimbs

The hindlimb is formed by bones: Pelvis, Femur, Patella, Tibia and Fibula, Tarsal bones, 3rd Metatarsus, 2nd and 4th metatarsus, proximal sesamoids, 1st phalanx (proximal), 2nd phalanx (middle), 3rd phalanx (distal) and distal sesamoid (navicular bone).

The pelvis is formed by the fusion of three bone pairs: Ilium, Ischium and Pubis, all are considered flat bones. Ilium presents the auricular surface where the sacrum is articulated. Between the Ischia and Ilium is the acetabulum, where the femur is articulated.

The equine femur has as its particularity the third trochanter, in the lateral direction. It is a long bone, it is articulated to the Coxal, Patella and Tibia. Performs the front and back movement of the animal's limb. The patella is a sesamoid bone of irregular shape and has the function of protecting the ligaments of the femur joint.

The Tibia and Fibula bones are fused together, the Fibula is needle-shaped and extends to the middle of Tibia's body. The tibia is a long bone and joins the fibula, femur, and tarsal bones. They perform the up and down movement of the leg.

The Tarsus is composed of the Talus, Calcaneus, Central, 1st and 2nd Tarsal bones (which are fused), 3rd Tarsal and 4th Tarsal. Together they form the anatomical region called the Hock. They participate in the leg up and down movement. All have an irregular shape, with the calcaneus bone being the largest among them, the talus is the second largest and has a cuboid shape just like the others. The 1st and 2nd Tarsal are fused.

The horses have the 2nd Metatarsal, 3rd Metatarsal and 4th Metatarsal bones. The biggest of all is the 3rd, with the 2nd and 4th stretching only halfway up the body. They are called long, irregular bones. They are articulated to the tarsal bones, sesamoid, and proximal phalanx.

The hindlimb of the horse is responsible for supporting 42% of the body mass¹⁴. The shape of this limb allows it to play a crucial role in longitudinal propulsion. The muscles are responsible for providing the necessary work for acceleration and for raising the center of mass when moving uphill^{12,19}. Many of the muscles of the hindlimbs are multiarticular and have several fascial connections, which makes it difficult to distinguish between intrinsic and extrinsic muscles¹⁷. Proximally, the pelvic limb is characterized by large muscular volumes and long fascicles, while more distally, the muscular component presents small and strained volumes and fascicles. In general, the proximal musculature is more specialized in generating work, while the distal musculature is generating economic strength¹⁹.

Figures 4 and 5 show the anatomical marks of the segments: pelvis, femur, tibia and fibula, metatarsal, hind pastern (P1 + P2), hind hoof (P3 + navicular bone) and their respective reflective markers (46 marks) proposed in the construction of the three-dimensional

biomechanical model proposed in this technical note. The markers were placed on the forelegs on the left right side of the horse.

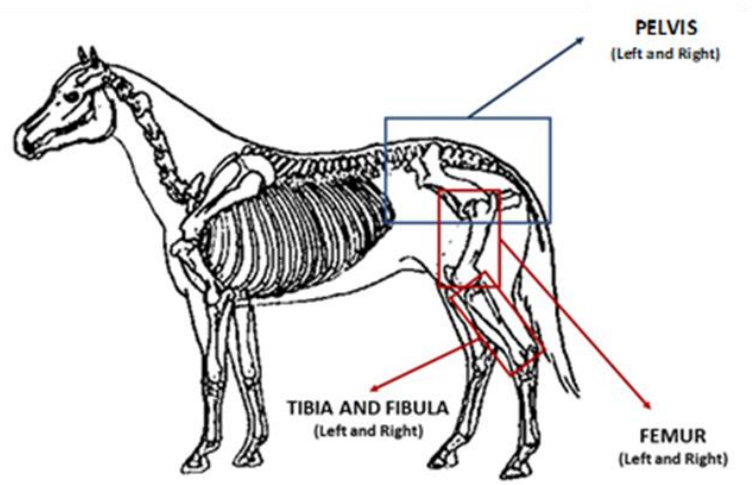


Figure 4: Hindlimb upper segments: Pelvis, Femur and Tibia and Fibula in the Equine Three-dimensional Biomechanics Model. Source: *EquiPERFORM project data* , 2022.

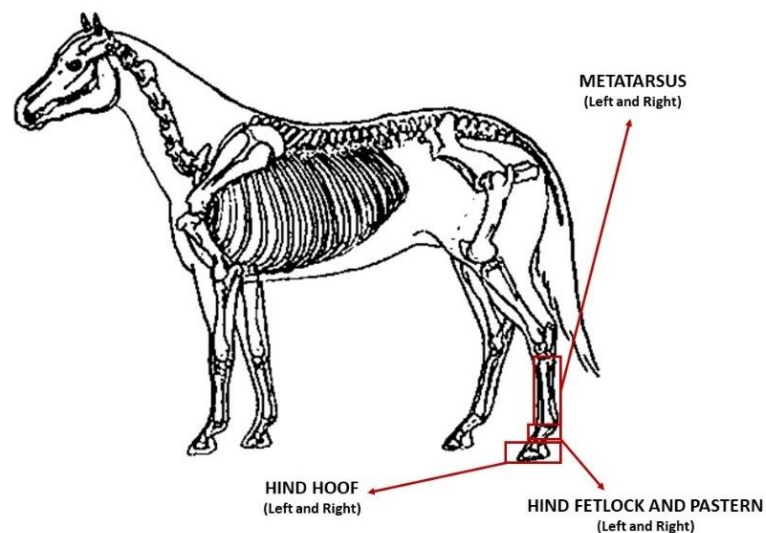


Figure 5: Hindlimb lower segments: Metatarsus, Pastern (Hind P1 + P2) and Hind Hoof in the Equine Three-dimensional Biomechanics Model. Source: *EquiPERFORM project data* , 2022

4. The equine's morphology and the rigid bodies of the biomechanical model

The models of morphological segments have an adjustable complexity depending on the total number of considered segments and the anatomical structures (skeletal, muscular and articular system). In the kinematic analysis, each segments of the model are represented by a

rigid body. Depending on the movement analyzed, one can have several rigid bodies, resulting in multi-segment models. For these reason a model can be studied, for instance, as, a Full body, an Forelimb, a Hindlimb, a Single Joint. This modeling process allows to represent the anatomical model by a similar mechanical set of segment. Therefore, the definition of the rigid bodies has to remain faithful to the morphology but also respect the mechanical characteristics of the system to be created. This morphological and mechanical adjustment "gives" the biomechanical model and the consequent source of kinematic data its own characteristics. To avoid mismatches between morphology and mechanics, proper placement of the markers is very important. Also the way the segments are aligned in space and articulated can influence the aforementioned data source, in particular, match a mechanical joint with the same number of degrees of freedom as the horse joint.

A rigid body in three-dimensional space has six degrees of freedom of movement, which means that six independent coordinates are needed to describe its position and orientation in this space³⁰. The six coordinates required to determine the position and orientation of the body can be, among others, the three coordinates of the position vector of the center of mass of the body and the three angles of rotation of a coordinate system fixed to the body under study, with a certain coordinate system, for example, attached to the laboratory. It is also known that when determining the spatial coordinates of three non-collinear points fixed to the rigid body, we obtain nine coordinates and three links (distances between points) sufficient to position it and orient it in space. In order to understand the movements that the horse makes when making movements, it is first necessary to understand the types of mobile joints in its body, the planes and axes in which they move and their degrees of freedom.

These six degrees of freedom are the three Cartesian coordinates and the three angles of rotation, which were referred, in this case, to the Euler angles. To identify these Cartesian coordinates, the three-dimensional position of at least three non-collinear points in each segment is required. The non-collinear points are the position of markers.

How joints can be described in terms of degrees of freedom, that is, the number of planes and axes they can move. A monoaxial joint has an axis and a plane, and therefore has a degree of freedom as shown in the Metacarpophalangeal joint of the figure 6 , the metacarpophalangeal joint as an example of this type of joint. A triaxial joint, where it presents three axes of movement and 3 three planes, resulting in three three degrees of freedom as shown in the hip joint figure.

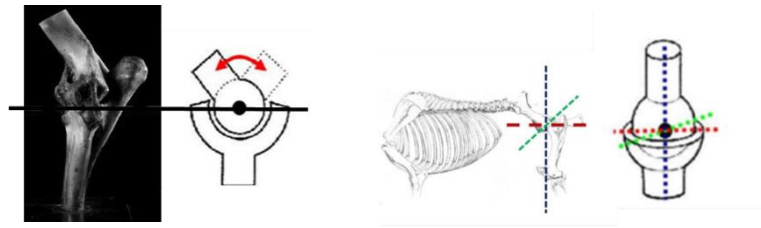


Figure 6: On the left, the metacarpophalangeal joint with 1 degree of freedom. On the right, the Hip joint with 3 degrees of freedom. (Pictures adapted from Museum of Veterinary Anatomy of the Faculty of Veterinary Medicine and Animal Science at Univ S. Paulo. Drawings from MovLab).

4.1. The skeleton and the placement of the reflective markers

These markers could be placed over predetermined anatomical regions and can be attached to the skin or directly attached to the bone. To study the location of the markers, EquiPerFORM used a horse skeleton from the Faculty of Veterinary Medicine of Universidade Lusófona. This skeleton was moved to Movlab to assist the team in making the decision about the location of these reflective markers as shown in figure. The markers used are spherical with 12mm in diameter fixed to the horses' skin with adhesive tape, so that their circular shape is maintained when viewed from different angles:



Figure: Representation of the set of full body markers on the horse's skeleton. The markers selected in the highlighted landmarks on the left side of the horse represent the same scheme on the right side. *Source: EquiPERFORM project data January 2020*

After defining the position of each marker on the skeleton, these were glued to the bony horse. When these are placed on the skin to represent the movement of the skeleton, it is

impossible to avoid the movement of the skin and subcutaneous tissue on the skeleton during the horse's gait. However, the expert collaboration of a veterinarian with precise knowledge of the horse's anatomy is important for the correct placement of the markers on the horse's surface to reliably represent the defined locations for the chosen placements on the skeleton.

4.2 Definition of 3D mechanical segments orientation for data collection

The origin of each local reference frame for each segment defined by the three-dimensional kinematic model is an intersection of three axes (X, Y and Z), registered according to the following items below:

Z - axis: vector longitudinal to the segment. In cases where segment is composed by 4 or more reflective markers the orientation of the longitudinal axis is defined as the vector that passes by the mid-point determined by both proximal markers and by the mid-point defined by both distal markers, instead, if segment is composed by 3 reflective markers, z-axis is defined as the vector with the orientation of the vector that crosses the lateral markers of the segment and which passes by the mid-point determined by the distal markers of the segment;

X - axis: vector pointing in a caudal→cranial direction. In cases where segment is composed by 4 or more reflective markers, the orientation of caudal → cranial vector is defined as the vectorial product between the longitudinal axis and the vector that goes through the mid-point determined by the lateral markers and by the mid-point determined by the medial markers in a four marker segment, instead, if segment is composed by 3 reflective markers, x-axis is defined as the vector with the orientation of the vectorial product between the longitudinal axis and the vector that passes through mid-point determined by the distal markers of the segment;

Y – axis: Vector pointing in a lateral→medial direction. Regardless segment is composed by 3 or more segments, this vector has the orientation of the vector defined by the vectorial product between the latter axes (Z and X axis).

The 26 segments of the full body are divided in three different groups: Head, Neck and Trunk; Forelimbs; Hindlimbs. Each one is described in the forward text.

5. Markers set and 3D segments orientation for data collection

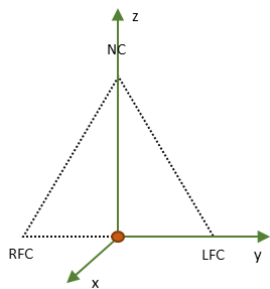
In MovLab model proposed, it will be defined as full body, represented by 103 reflective markers, allowing to define 26 different segments (that include: head, neck, trunk, left scapula, right scapula, left humerus, right humerus, left radius and ulna, right radius and ulna, left metacarpus, right metacarpus, left fore fetlock and pastern (fore P1 + P2), right fore fetlock and

pastern (fore P1 + P2), left fore hoof, right fore hoof, pelvis, left femur, right femur, left tibia and fibula, right tibia and fibula, left metatarsus, right metatarsus, left hind fetlock and pastern (hind P1 + P2), right hind fetlock and pastern (hind P1 + P2), left hind hoof and right hind hoof).

The multi markers set is based on the marker anatomical reference. This association will be the basic spatial framework of reference to reconstruct the 3D model. The 3D segments spatial orientation for data collection will depends of those references axis which in turn depends on the precise marker anatomical position. The next tables show the orientation of the three-dimensional spatial of all the segments proposed in the present model.

5.1 Segment: Head

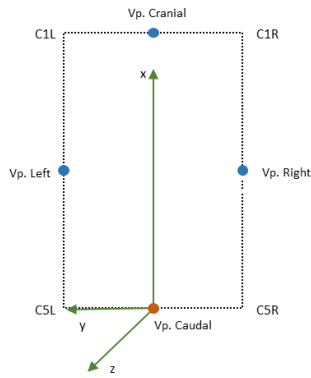
Anatomical Segment	Marker Name	Marker Anatomical Reference
HEAD	NC	Nucal Crest
	LFC	Left Facial Crest (cranial)
	RFC	Right Facial Crest (cranial)



Origin	MidPoint (LFC, RFC, NC)
X	Perpendicular to the plan create with NC, MidPoint and FCL
Y	MidPoint → FCL
Z	MidPoint → NC

5.2 Segment: Neck

Anatomical Segment	Marker Name	Marker Anatomical Reference
NECK	C1L	Left Cranial portion of the atlas wing
	C1R	Right Cranial portion of the atlas wing
	C5L	Left Transverse Process of the C5
	C5R	Right Transverse Process of the C5



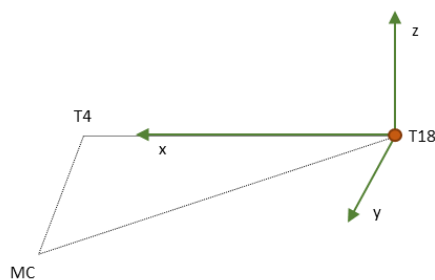
Origin	Vp. Caudal
X	Vp. Caudal → Vp. Cranial
Y	Perpendicular to Z and X
Z	Perpendicular to the plan create with vp caudal, vp cranial and C5R

5.3 Segment: Trunk (Body) and the three parts: thorax, back spine, and tail

Anatomical Segment	Marker Name	Marker Anatomical Reference
TRUNK (BODY)	T4	Spinous Process of the T4
	T18	Spinous Process of the T18
	L6	Spinous Process of the L6
	S1	Spinous Process of the S1
	CC	Coccygeal Vertebrae
	MC	Manubrial Cartilage

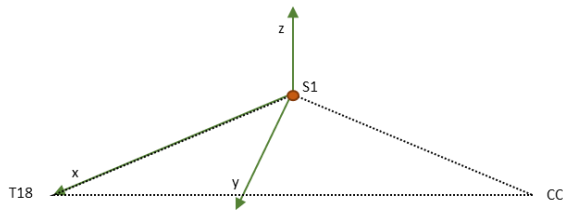
The trunk is divided in three parts: thorax, back spine, and tail.

Thorax:



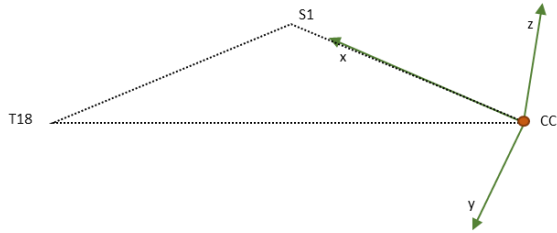
Origin	T18
X	T18 → T4
Y	Perpendicular to plan create with T4, T18 and MC
Z	Perpendicular to X and Y

Back spine



Origin	S1
X	$S1 \rightarrow T18$
Y	Perpendicular to the plan create with T18, S1 and CC
Z	Perpendicular to X and Y

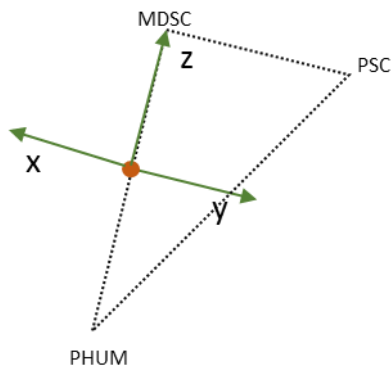
Tail:



Origin	CC
X	$CC \rightarrow S1$
Y	Perpendicular to the plan create with T18, S1 and CC
Z	Perpendicular to X and Y

5.4 Segment: Scapula

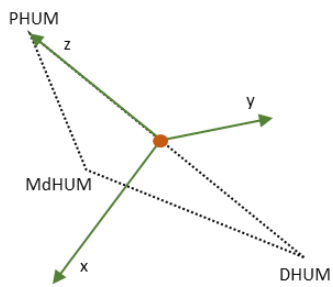
Anatomical Segment	Marker Name	Marker Anatomical Reference
SCAPULA - LEFT	LPSC	Left Caudal Dorsal Border of the Scapula
	LMdSC	Left Tuberosity of the scapula spine (on the flattest area)
	LCHUM	Left Cranial Part of the greater tubercle of the humerus
SCAPULA - RIGHT	RPSC	Right Caudal Dorsal Border of the Scapula
	RMdSC	Right Tuberosity of the scapula spine (on the flattest area)
	RCHUM	Right Cranial Part of the greater tubercle of the Humerus



Origin	Midpoint between MDSC and PHUM
X	Perpendicular to Z and Y
Y	Perpendicular to the plan create with midpoint, PSC and MDSC
Z	Midpoint → MDSC

5.5 Segment: Humerus

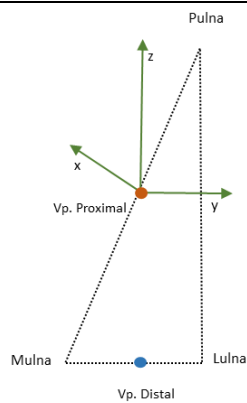
Anatomical Segment	Marker Name	Marker Anatomical Reference
HUMERUS - LEFT	LCHUM	Left Cranial Part of the greater tubercle of the humerus
	LDHUM	Left Lateral Epicondyle of the humerus
	LMdHUM	Left Deltoid Tuberosity of the humerus
HUMERUS - RIGHT	RCHUM	Right Cranial Part of the greater tubercle of the Humerus
	RDHUM	Right Lateral Epicondyle of the Humerus
	RMdHUM	Right Deltoid Tuberosity of the Humerus



Origin	Midpoint between PHUM and DHUM
X	Perpendicular to Z and Y
Y	Perpendicular to the plan create with midpoint, PHUM and MdhUM
Z	Midpoint → PHUM

5.6 Segment: Radius and Ulna

Anatomical Segment	Marker Name	Marker Anatomical Reference
RADIUS AND ULNA - LEFT (FOREARM)	LPULNA	Left Lateral Coronoid Process of the Ulna
	LLULNA	Left Lateral Styloid Process
	LMULNA	Left Medial Styloid Process
	LACC	Palmar Border of the Left Accessory carpal bone
RADIUS AND ULNA - RIGHT (FOREARM)	RPULNA	Right Lateral Coronoid Process of the Ulna
	RLULNA	Right Lateral Styloid Process
	RMULNA	Right Medial Styloid Process
	RACC	Palmar Border of the Right Accessory carpal bone

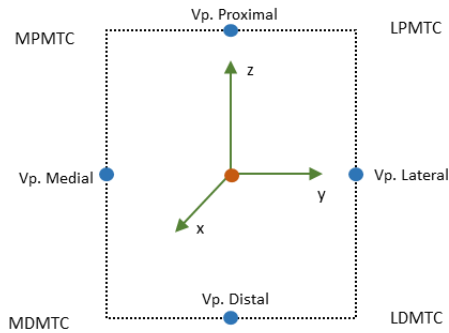


Origin	MidPoint between PULNA and MULNA
X	Perpendicular to the plan create with vp proximal, MULNA and LULNA
Y	Perpendicular to Z and X
Z	Vp distal → Vp proximal

5.7 Segment: Metacarpus

Anatomical Segment	Marker Name	Marker Anatomical Reference
METACARPUS - LEFT	LLPMTC	Left Proximal Extremity of the interosseous space between IV and III metacarpus
	LLDMTC	Left Distal Extremity of the IV metacarpus
	LMDMTC	Left Distal Extremity of the II metacarpus
	LMPMTC	Left Proximal Extremity of the interosseous space between II and III metacarpus
	LFSES	Left – Palmar to the intersesamoidean space
	RLPMTC	Right Proximal Extremity of the interosseous space between IV and III metacarpus

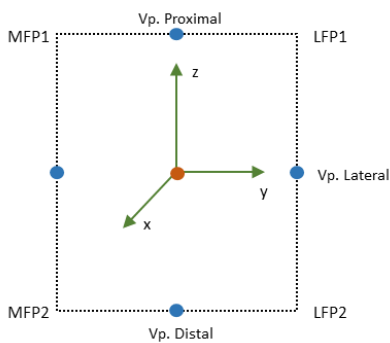
METACARPUS - RIGHT	RLDMTC	Right Distal Extremity of the IV metacarpus
	RMDMTC	Right Distal Extremity of the II metacarpus
	RMPMTC	Right Proximal Extremity of the interosseous space between II and III metacarpus
	RFSES	Right – Palmar to the intersesamoidean space



Origin	MidPoint between Vp. Proximal and Vp. Distal
X	Perpendicular to the plan create with vp proximal, vp. Lateral and vp. Medial
Y	Perpendicular to Z and X
Z	Midpoint (Origin) → Vp proximal

5.8 Segment: Fore Pastern (P1+P2)

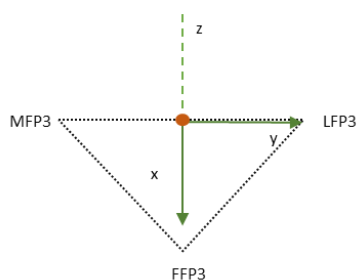
Anatomical Segment	Marker Name	Marker Anatomical Reference
PASTERN – LEFT (FORE P1 + P2)	LLFP1	Left – Lateral proximal tuberosity of P1
	LLFP2	Left – Lateral proximal tuberosity of P2
	LMFP2	Left – Medial proximal tuberosity of P2
	LMFP1	Left – Medial proximal tuberosity of P1
PASTERN – RIGHT (FORE P1 + P2)	RLFP1	Right – Lateral proximal tuberosity of P1
	RLFP2	Right – Lateral proximal tuberosity of P2
	RMFP2	Right – Medial proximal tuberosity of P2
	RMFP1	Right – Medial proximal tuberosity of P1



Origin	MidPoint between Vp. Proximal and Vp. Distal
X	Perpendicular to the plan create with vp proximal, vp. Lateral and vp. Medial
Y	Perpendicular to Z and X
Z	Midpoint (Origin) → Vp proximal

5.9 Segment: Fore Hoof

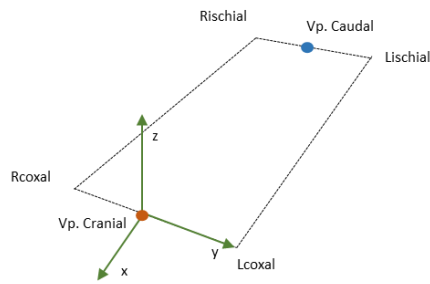
Anatomical Segment	Marker Name	Marker Anatomical Reference
FORE HOOF - LEFT	LLFP3	Left – Quarter at the level of lateral palmar process of P3
	LMFP3	Left – Quarter at the level of medial palmar process of P3
	LFFP3	Left – 1cm below the coronary band (extensor process of P3)
	LFFDP3	Left – 3cm distal to LFFP3
FORE HOOF - RIGHT	RLFP3	Right – Quarter at the level of lateral palmar process of P3
	RMFP3	Right – Quarter at the level of medial palmar process of P3
	RFFP3	Right – 1cm below the coronary band (extensor process of P3)
	RFFDP3	Right – 3cm distal to RFFP3



Origin	MidPoint between MFP3 and LFP3
X	Midpoint (origin) → FFP3
Y	Perpendicular to Z and X
Z	Perpendicular to the plan create with MFP3, LFP3 and FFP3

5.10 Segment: Pelvis

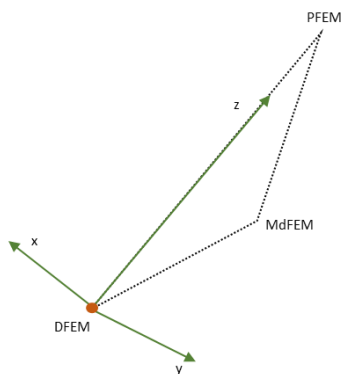
Anatomical Segment	Marker Name	Marker Anatomical Reference
PELVIS - LEFT	LCoxal	Left – Caudovernal Extremity of the coxal tuber
	LIschial	Left – Ischial tuber
PELVIS - RIGHT	RCoxal	Right – Caudovernal Extremity of the coxal tuber
	RIschial	Right – Ischial tuber



Origin	Midpoint between RCOXAL and LCOXAL (Vp. Cranial)
X	Perpendicular to Z and Y
Y	Vp. Cranial → LCOXAL
Z	Perpendicular to the plan create with LCOXAL, vp. Caudal and Vp. Cranial

5.11 Segment: Femur

Anatomical Segment	Marker Name	Marker Anatomical Reference
FEMUR - LEFT	LPFEM	Left – Greater trochanter of the femur
	LDFEM	Left – Lateral Epicondyle of the Femur
	LMdFEM	Left – Middle distance between marker LPFEM and LDFEM
FEMUR - RIGHT	RPFEM	Right – Greater trochanter of the femur
	RDFEM	Right – Lateral Epicondyle of the Femur
	RMdFEM	Right – Middle distance between marker RPFEM and RDFEM

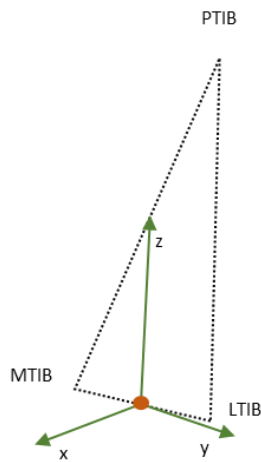


Origin	DFEM
X	Perpendicular to X and Z
Y	Perpendicular to the plan create with DFEM, MdfFEM and PFEM
Z	DFEM → PFEM

5.12 Segment: Tibia and Fibula

Anatomical Segment	Marker Name	Marker Anatomical Reference
	LPTIB	Left Tibial Tuberosity

TIBIA & FIBULA - LEFT	LMDTIB	Left – Middle distance between marker LPTIB and LLTIB
	LLTIB	Left – Proximal to the lateral malleolus of the Fibula
	LMTIB	Left – 2cm proximal to the medial malleolus of the Tibia
TIBIA & FIBULA - RIGHT	RPTIB	Right Tibial Tuberosity
	RMdTIB	Right – Middle distance between marker RPTIB and RLtIB
	RLTIB	Right – Proximal to the lateral malleolus of the Fibula
	RMTIB	Right – 2cm proximal to the medial malleolus of the Tibia

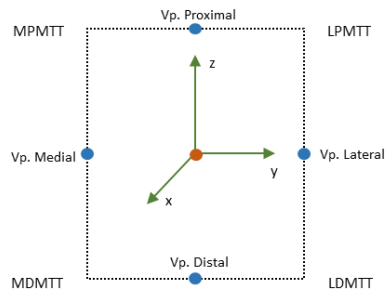


Origin	MidPoint between MTIB and LTIB
X	Perpendicular to the plan with MTIB, LTIB and PTIB
Y	Perpendicular to Z and X
Z	Direction from LTIB to PTIB starting in the Vp. Distal

5.13 Segment: Metatarsus

Anatomical Segment	Marker Name	Marker Anatomical Reference
METATARSUS - LEFT	LLPMTT	Left Proximal Extremity of the interosseous space between IV and III metatarsus
	LLDMTT	Left – Distal Extremity of the IV Metatarsus
	LHSES	Left – Plantar to the intersesamoidean space
	LMDMTT	Left – Distal Extremity of the II Metatarsus
	LMPMTT	Left - Proximal Extremity of the interosseous space between II and III metatarsus
	RLPMTT	Right Proximal Extremity of the interosseous space between IV and III metatarsus

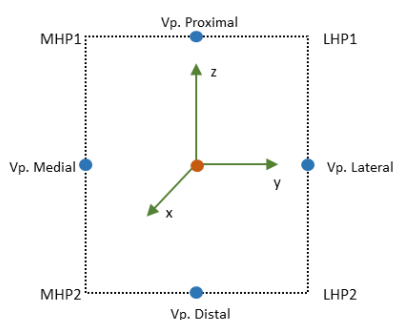
METATARSUS - RIGHT	RLDMTT	Right – Distal Extremity of the IV Metatarsus
	RHSES	Right – Plantar to the intersesamoidean space
	RMDMTT	Right – Distal Extremity of the II Metatarsus
	RMPMTT	Right - Proximal Extremity of the interosseous space between II and III metatarsus



Origin	MidPoint between Vp. Proximal and Vp. Distal
X	Perpendicular to the plan create with vp proximal, vp. Lateral and vp. Medial
Y	Perpendicular to Z and X
Z	Midpoint (Origin) → Vp proximal

5.14 Segment: Hind Pastern (P1+P2)

Anatomical Segment	Marker Name	Marker Anatomical Reference
PASTERN – LEFT (HIND P1 + P2)	LLHP1	Left – Lateral proximal tuberosity of P1
	LLHP2	Left – Lateral proximal tuberosity of P2
	LMHP2	Left – Medial proximal tuberosity of P2
	LMHP1	Left – Medial proximal tuberosity of P1
PASTERN – RIGHT (HIND P1 + P2)	RLHP1	Right – Lateral proximal tuberosity of P1
	RLHP2	Right – Lateral proximal tuberosity of P2
	RMHP2	Right – Medial proximal tuberosity of P2
	RMHP1	Right – Medial proximal tuberosity of P1

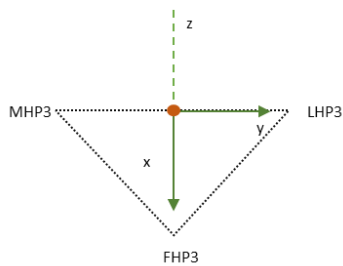


Origin	MidPoint between Vp. Proximal and Vp. Distal
X	Perpendicular to the plan create with vp proximal, vp. Lateral and vp. Medial
Y	Perpendicular to Z and X
Z	MidPoint (Origin) → Vp proximal

5.15 Segment: Hind Hoof (left; right)

Anatomical Segment	Marker Name	Marker Anatomical Reference
HIND HOOF - LEFT	LLHP3	Left – Quarter at the level of lateral palmar process of P3
	LMHP3	Left – Quarter at the level of medial palmar process of P3
	LFHP3	Left – 1cm below the coronary band (extensor process of P3)
	LHFDP3	Left – 3cm distal to LFHP3

HIND HOOF - RIGHT	RLHP3	Right – Quarter at the level of lateral palmar process of P3
	RMHP3	Right – Quarter at the level of medial palmar process of P3
	RFHP3	Right – 1cm below the coronary band (extensor process of P3)
	RHFDP3	Right – 3cm distal to RFHP3



Origin	MidPoint between MFP3 and LHP3
X	Midpoint (origin) → FHP3
Y	Perpendicular to Z and X
Z	Perpendicular to the plan create with MHP3, LHP3 and FHP3

6. Joints angular references based on the relative 3D orientation

The relative spatial orientation of the references axis 3D for each angular position depends on the instantaneous center of rotation common two adjacent bodies. The center of rotation is the point that has zero angular velocity at any time during the movement. The spatial position of the center of rotation depends for each instant of the dot product of the longitudinal axis of the two adjacent bodies. The dot product for each instant (100 frames per second) depends of the computation availability but it gives some degree of certainty in determining the position of this center even if its position changes within the joint. In fact, the center of rotation remains in the same place, within the joint, if the rotation occurs at a constant radius of curvature of a given joint surface; however, if the radius is variable, the center of rotation moves according to a characteristic pattern of that joint^{7,8,9,10,11}.

The location of the instantaneous centers of rotation is extremely important for the measurement of the angular movements of the joints obtained from the methods of kinematic analysis, in which the skin markers are placed under their estimated location^{7,8,9,10,11}.

The joints vary in structure as well as the disposition of their elements and are often characterized by functions. However, they have certain structural and functional characteristics that can be classified into three types: fibrous joint – called synarthrosis; cartilaginous joints – called amphiarthrosis; and synovial articulation – called diarthrosis⁷.

Each joint of the model was modeled as having six degrees of freedom. This allows the calculation of anatomical movements (flexion/extension, adduction/abduction, and medial/lateral rotation) that are expressed as movements of the distal segment in relation to the proximal segment, considered as a reference segment. Table 4 and figures 7 to 9 presents the description of the joints of the body proposed in the model^{7,8,9,10,11}.



Figure 7 – Joints under study of the Equine three-dimensional Biomechanical Model using Vicon.

Table 4 – Joint of all segments in the Equine three-dimensional Biomechanical Model

	Anatomical Joint Designation	Joint Number	Type of Joint
BODY	Atlanto-Occipital Joint		
	Cervico-thoracic Joint		
	Lumbosacral Joint		
FORELIMBS	Left Distal Interphalangeal Joint (Forelimb) Right Distal Interphalangeal Joint (Forelimb)	1	
	Left Metacarpophalangeal Joint Right Metacarpophalangeal Joint	2	
	Left Carpal Joint Right Carpal Joint	3	
	Left Humeroradial Joint Right Humeroradial Joint	4	
	Left Scapulohumeral Joint Right Scapulohumeral Joint	5	
HINDLIMBS	Left Distal Interphalangeal Joint (Hindlimb) Right Distal Interphalangeal Joint (Hindlimb)	6	
	Left Metatarsophalangeal Joint Right Metatarsophalangeal Joint	7	
	Left Tarsal Joint Right Tarsal Joint	8	
	Left Femorotibial Joint Right Femorobial Joint	9	
	Left Coxofemoral Joint Right Coxofemoral Joint	10	

For the dot product calculation of this movements in each joint it is using the vectors of the two adjacent segments:

- **Flexion and extension:**

The flexion/extension movement is calculated from dot product of the longitudinal vectors of each segment, the Z axis. When the two Z axis of both segments cross to each other it is calculate the angle of that joint in that instant. If the distal segment (which is the moving

segment) makes an angle with the proximal segment in a cranial/dorsal position the angle will have positive values but if the angle of the two segments is made in a caudal/palmar/plantar position is going to have negative values as it shows in figure 7.

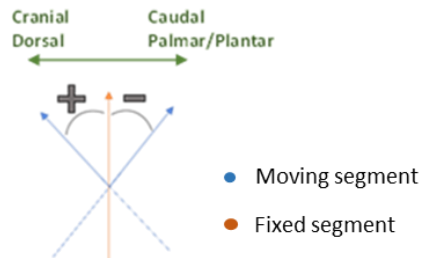


Figure 8 – Demonstration of the flexion/extension vectors for the joints.

- **Adduction/abduction:**

The adduction/abduction movement is calculated from is calculated from dot product of the cranio→caudal vectors of each segment, the X axis. When the movement is made to the medial side it goes in the positive direction and it is considered the adduction, and when the movement is made to the lateral side it goes in the negative direction and it is considered abduction.

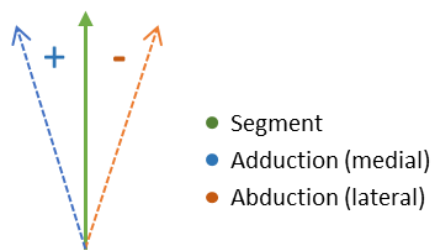


Figure 9 – Demonstration of the adduction/abduction vectors for the segment.

7. Model's vectors. Placement of markers. Joints movement patterns

Joint #1

The joint number 1 can be found in distal portion of the forelimbs and is anatomical designate as distal interphalangeal joint (DIJ) also known as coffin joint that is formed by the distal articular surface of the 2nd phalanx (middle), the articular surface of the 3rd phalanx and the two articular surfaces of the distal sesamoid bone (navicular bone).

In the present study the joint n^o 1 has two segments – 3rd phalanx and Pastern (P1+P2) with 4 markers in each segment as showed in table 5.

Table 5 – Description of the segments and markers of the joint number 1.

Joint Number	Related Segments	Segments Markers (Localization and acronym)
1	Forelimb 3 rd phalange (P3)	Quarter at the level of lateral palmar process of P3 - LFP3 Quarter at the level of medial palmar process of P3 - MFP3 1cm below the coronary band (extensor process of P3) - FFP3 3cm distal to FFP3 - FFDP3
	Forelimb Pastern (P1 + P2)	Lateral proximal tuberosity of P1 - LFP1 Lateral proximal tuberosity of P2 - LFP2 Medial proximal tuberosity of P2 - MFP2 Medial proximal tuberosity of P1 - MFP1

The figure 10 demonstrate the movement of the joint n^o 1 in the standing position and in slight flexion position with the vector of the Z axis of each segment (orange arrows). In this joint the standing position (figure 10a) demonstrate a positive initial number of the angle of this joint, in a flexion position (figure 10b) that angle becomes higher in a positive way.

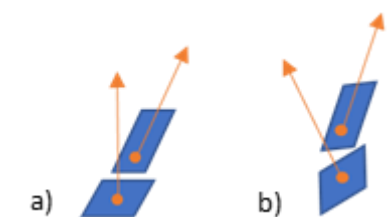


Figure 10 – Vectors of Z axis of each segment in the Joint n^o1.

a) standing position; b) slight flexion position

In the figure 11 it is shown a graphic of the sagittal plane's pattern of the joint nº1 which demonstrate the flexion and extension movement of this joint with the flexion in the positive values and the extension in the negative values. For the abduction/adduction and rotation movement we must find experimental plane's patterns plane's pattern.

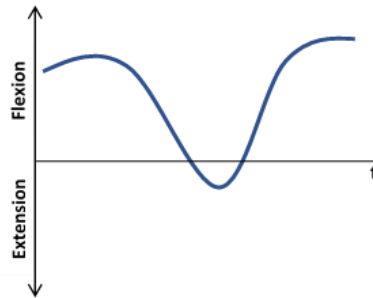


Figure 11 – Graphic of the sagittal plane's movement of the joint nº1 which shows the flexion/extension movement of this joint.

Joint #2

The joint number 2 can be found in distal portion of the forelimbs and is anatomical designate as metacarpophalangeal joint (MCP) that is formed by the distal articular surface of the 3rd metacarpus, the proximal articular surface of the proximal phalanx and the articular surface of the proximal sesamoid bones.

In the present study the joint nº 2 has two segments –Pastern (P1+P2) and 3rd metacarpus with 4 markers in the first segment and 5 markers in the second segment as showed in table 6.

Table 6 – Description of the segments and markers of the joint number 2.

Joint Number	Related Segments	Segments Markers (Localization and acronym)
2	Forelimb Pastern (P1 + P2)	Lateral proximal tuberosity of P1 - LFP1 Lateral proximal tuberosity of P2 - LFP2 Medial proximal tuberosity of P2 - MFP2 Medial proximal tuberosity of P1 - MFP1
	3 rd metacarpus	Proximal Extremity of the interosseous space between IV and III metacarpus - LPMTC Distal Extremity of the IV metacarpus - LDMTC Distal Extremity of the II metacarpus - MDMTC

		Proximal Extremity of the interosseous space between II and III metacarpus - MPMTC Palmar to the intersesamoidean space - LFSES
--	--	---

The figure 12 demonstrate the movement of the joint nº 2 in the standing position and in slight flexion position with the vector of the Z axis of each segment (orange arrows). In this joint the standing position (figure 12a) shows a negative initial number of the angle of this joint and in a flexion position (figure 12b) that angle becomes bigger leading to positive numbers.

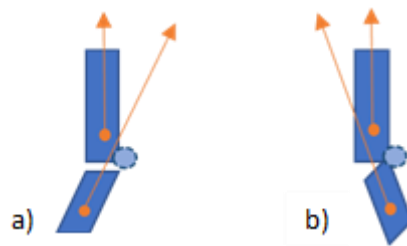


Figure 12 – Vectors of Z axis of each segment in the Joint nº2.

a) standing position; b) slight flexion position

In the figure 13 it is shown a graphic of the sagittal plane's movement of the joint nº2 which demonstrate the flexion and extension movement of this joint with the flexion in the positive values and the extension in the negative values.

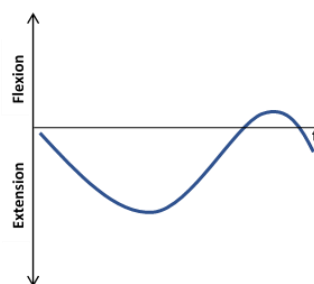


Figure 13 – Graphic of the sagittal plane's movement of the joint nº2 which shows the flexion/extension movement of this joint.

Joint #3

The joint number 3 can be found in distal portion of the forelimbs and is anatomical designate as carpal joint that is a compound joint composed of the radius and ulna proximally, six carpal bones, and the fused 3rd and 4th metacarpal bones distally. The carpal bones are arranged in two rows, the proximal row consists of the accessory, ulnar, intermediate, and radial carpal bones.

In the present study the joint n^o 3 has two segments – 3rd metacarpus and radius and ulna with 5 markers in the first segment and 3 markers in the second segment as showed in table 7.

Table 7 – Description of the segments and markers of the joint number 3.

Joint Number	Related Segments	Segments Markers (Localization and acronym)
3	3 rd metacarpus	Proximal Extremity of the interosseous space between IV and III metacarpus - LPMTC Distal Extremity of the IV metacarpus - LDMTC Distal Extremity of the II metacarpus - MDMTC Proximal Extremity of the interosseous space between II and III metacarpus - MPMTC Palmar to the intersesamoidean space - LFSES
	Radius and ulna	Lateral Coronoid Process of the Ulna - PULNA Lateral Styloid Process - LULNA Medial Styloid Process - MULNA

The figure 14 demonstrate the movement of the joint n^o 3 in the standing position and in slight flexion position with the vector of the Z axis of each segment (orange arrows). In this joint the standing position (figure 14a) shows a neutral initial number around zero of the angles of this joint and in a flexion position (figure 14b) that angle increases towards positive numbers.

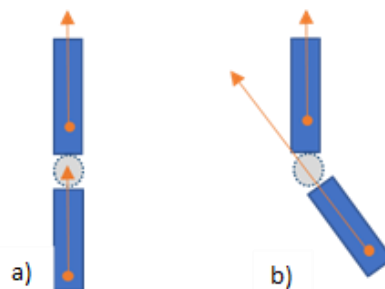


Figure 14 – Vectors of Z axis of each segment in the Joint n^o3.

a) standing position; b) slight flexion position

In the figure 15 it is shown a graphic of the sagittal plane's movement of the joint nº3 which demonstrate the flexion and extension movement of this joint with the flexion in the positive values and the extension in values around zero. Because of the anatomical characteristics the maximum of extension for this joint is around zero as we can see in the figure 14a and figure 15.

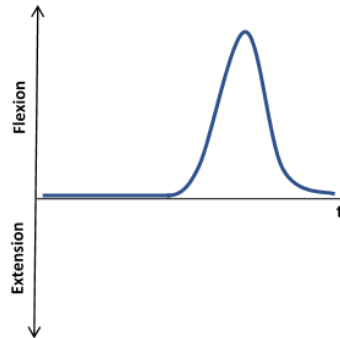


Figure 15 – Graphic of the sagittal plane's movement of the joint nº3 which shows the flexion/extension movement of this joint.

Joint #4

The joint number 4 can be found in proximal portion of the forelimbs and is anatomical designate as humero-radio-ulnar joint also known as elbow joint that is formed by the distal portion of the humerus and the proximal portion of radius and ulna.

In the present study the joint n^o 4 has two segments – radius and ulna and humerus with 3 markers in each segment as showed in table 8.

Table 8 – Description of the segments and markers of the joint number 4.

Joint Number	Related Segments	Segments Markers (Localization and acronym)
4	Radius and ulna	Lateral Coronoid Process of the Ulna - PULNA Lateral Styloid Process - LULNA Medial Styloid Process - MULNA
	Humerus	Cranial Part of the greater tubercle of the humerus - CHUM Deltoid Tuberosity of the humerus - MdHUM Lateral Epicondyle of the humerus - DHUM

The figure 16 demonstrate the movement of the joint n^o 4 in the standing position and in slight flexion position with the vector of the Z axis of each segment (orange arrows). In this joint the standing position (figure 16a) gives us an initial negative number of the angle of this joint and in a flexion position (figure 16b) that angle decrease to more negative numbers.

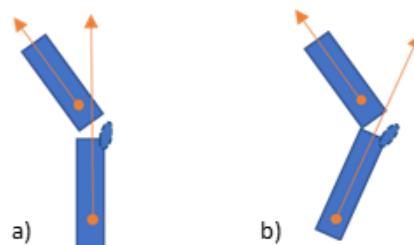


Figure 16 – Vectors of Z axis of each segment in the joint n^o4.

a) standing position; b) slight flexion position

In the figure 17 it is shown a graphic of the sagittal plane's movement of the joint nº4 which demonstrate the flexion and extension movement of this joint with the flexion in the negative values and the extension in the positive values. Due to the morphology in this joint it is not possible to achieve the positive values as it is demonstrated in the figure 16 and 17.

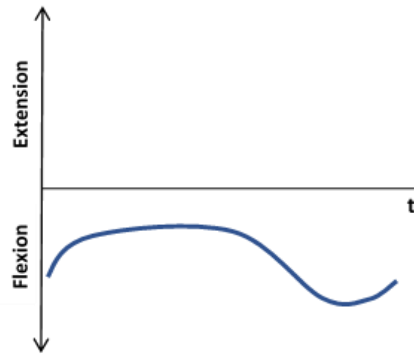


Figure 17 – Graphic of the sagittal plane's movement of the joint nº4 which shows the flexion/extension movement of this joint.

Joint #5

The joint number 5 can be found in proximal portion of the forelimbs and is anatomical designate as scapula-humeral joint

In the present study the joint nº 5 has two segments – humerus and scapula with 3 markers in each segment as showed in table 9.

Table 9 – Description of the segments and markers of the joint number 5.

Joint Number	Related Segments	Segments Markers (Localization and acronym)
5	Humerus	Cranial Part of the greater tubercle of the humerus - CHUM Deltoid Tuberosity of the humerus - MdHUM Lateral Epicondyle of the humerus - DHUM
	Scapula	Cranial Part of the greater tubercle of the humerus - CHUM

		Tuberosity of the scapula spine (on the flattest area) - MdSC Caudal Dorsal Border of the Scapula - PSC
--	--	---

The figure 18 demonstrate the movement of the joint nº 5 in the standing position and in slight flexion position with the vector of the Z axis of each segment (orange arrows). In this joint the standing position (figure 18a) has an initial positive number of the angle and in a flexion position (figure 18b) that angle stays in the positive with higher values.

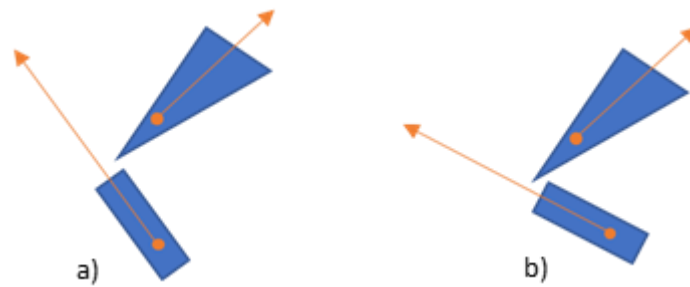


Figure 18 – Vectors of Z axis of each segment in the joint nº 5.

a) standing position; b) slight flexion position

In the figure 19 it is shown a graphic of the sagittal plane's movement of the joint nº5 which demonstrate the flexion and extension movement of this joint with the flexion in the positive values and the extension in the negative values. Due to the morphology of this joint it is not possible to achieve the negative values as demonstrated in the figure 18 and 19.

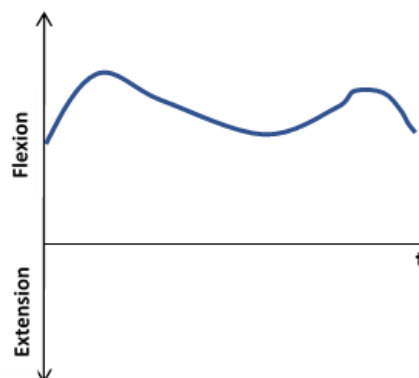


Figure 19 – Graphic of the sagittal plane's movement of the joint nº5 which shows the flexion/extension movement of this joint.

Joint #6

The joint number 6 can be found in distal portion of the hindlimbs and is anatomical designate as distal interphalangeal joint (DIJ) also known as coffin joint that is formed by the distal articular surface of the 2nd phalanx (middle), the articular surface of the 3rd phalanx and the two articular surfaces of the distal sesamoid bone (navicular bone).

In the present study the joint n^o 6 has two segments – 3rd phalanx and Pastern (P1+P2) of the hindlimbs with 4 markers in each segment as showed in table 10.

Table 10 – Description of the segments and markers of the joint number 6.

Joint Number	Related Segments	Segments Markers (Localization and acronym)
6	Hindlimb 3 rd phalanx (P3)	Quarter at the level of lateral palmar process of P3 - LHP3 Quarter at the level of medial palmar process of P3 - MHP3 1cm below the coronary band (extensor process of P3) - FHP3 3cm distal to FHP3 - FHDP3
	Hindlimb Pastern (P1 + P2)	Lateral proximal tuberosity of P1 - LHP1 Lateral proximal tuberosity of P2 - LHP2 Medial proximal tuberosity of P2 - MHP2 Medial proximal tuberosity of P1 - MHP1

The figure 20 demonstrate the movement of the joint n^o 1 in the standing position and in slight flexion position with the vector of the Z axis of each segment (orange arrows). In this joint the standing position (figure 20a) gives us a positive initial number of the angle of this joint, in a flexion position (figure 20b) that angle becomes bigger in a positive way.

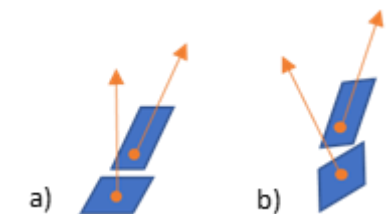


Figure 20 – Vectors of Z axis of each segment in the joint n^o 6.

a) standing position; b) slight flexion position

In the figure 21 it is shown a graphic of the sagittal plane's movement of the joint n^o6 which demonstrate the flexion and extension movement of this joint with the flexion in the positive values and the extension in the negative values.

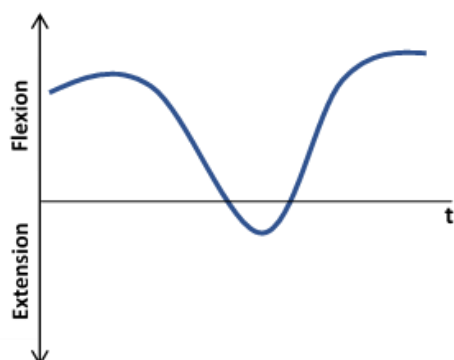


Figure 21 – Graphic of the sagittal plane's movement of the joint n^o6 which shows the flexion/extension movement of this joint.

Joint #7

The joint number 7 can be found in distal portion of the forelimbs and is anatomical designate as metacarpophalangeal joint (MCP) that is formed by the distal articular surface of the 3rd metatarsus, the proximal articular surface of the proximal phalanx and the articular surface of the proximal sesamoid bones.

In the present study the joint n^o 2 has two segments –Pastern (P1+P2) and 3rd metatarsus with 4 markers in the first segment and 5 markers in the second segment as showed in table 6.

Table 11 – Description of the segments and markers of the joint number 7.

Joint Number	Related Segments	Segments Markers (Localization and acronym)
VII	Hindlimb Pastern (P1 + P2)	Lateral proximal tuberosity of P1 - LHP1 Lateral proximal tuberosity of P2 - LHP2 Medial proximal tuberosity of P2 - MHP2 Medial proximal tuberosity of P1 - MHP1
	3 rd metatarsus	Proximal Extremity of the interosseous space between IV and III metatarsus - LPMTT Distal Extremity of the IV Metatarsus - LDMTT Plantar to the intersesamoidean space - LHSES Distal Extremity of the II Metatarsus - MDMTT

		Proximal Extremity of the interosseous space between II and III metatarsus - MPMTT
--	--	---

The figure 22 demonstrate the movement of the joint nº 2 in the standing position and in slight flexion position with the vector of the Z axis of each segment (orange arrows). In this joint the standing position (figure 22a) gives us a negative initial number of the angle of this joint and in a flexion position (figure 22b) that angle becomes bigger leading to positive numbers.

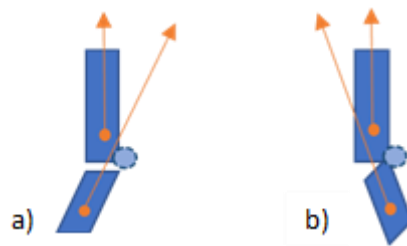


Figure 22 – Vectors of Z axis of each segment in the joint nº 7.

a) standing position; b) slight flexion position

In the figure 23 it is shown a graphic of the sagittal plane’s movement of the joint nº7 which demonstrate the flexion and extension movement of this joint with the flexion in the positive values and the extension in the negative values.

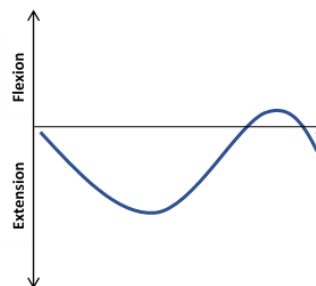


Figure 23 – Graphic of the sagittal plane’s movement of the joint nº7 which shows the flexion/extension movement of this joint.

Joint #8

The joint number 8 can be found in distal portion of the forelimbs and is anatomical designate as the tarsus also known as the hock. This joint consists of three rows leading to four smaller joints: the tibiotarsal joint, the proximal intertarsal joint, the distal intertarsal joint and the tarsometatarsal joint. That are formed by the distal articular surface if the tibia, the talus bone, the calcaneous bone, the central tarsal bone, the first and second tarsal bones (fused), the third tarsal bone, the fourth tarsal bone and the proximal articular surface of the third and second metatarsal bones.

In the present study the joint nº 8 has two segments – 3rd metatarsus and tibia and fibula with 5 markers in the first segment and 4 markers in the second segment as showed in table 12.

Table 12 – Description of the segments and markers of the joint number 8.

Joint Number	Related Segments	Segments Markers (Localization and acronym)
8	3 rd metatarsus	Proximal Extremity of the interosseous space between IV and III metatarsus - LPMTT Distal Extremity of the IV Metatarsus - LDMTT Plantar to the intersesamoidean space - LHSES Distal Extremity of the II Metatarsus - MDMTT Proximal Extremity of the interosseous space between II and III metatarsus - MPMTT
	Tibia and Fibula	Tibial Tuberosity - PTIB Middle distance between marker PTIB and LTIB - MdTIB Proximal to the lateral malleolus of the Fibula - LTIB 2cm proximal to the medial malleolus of the Tibia - MTIB

The figure 24 demonstrate the movement of the joint nº 8 in the standing position and in slight flexion position with the vector of the Z axis of each segment (orange arrows). In this joint the standing position (figure 24a) gives us a negative initial number of the angle of this joint and in a flexion position (figure 24b) that angle becomes even more negative.

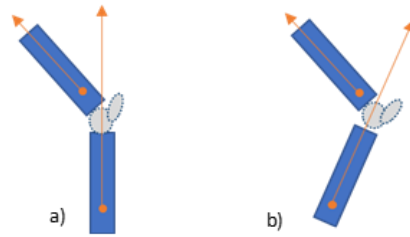


Figure 24 – Vectors of Z axis of each segment in the joint n° 8.

a) standing position; b) slight flexion position

In the figure 25 it is shown a graphic of the sagittal plane’s movement of the joint n°8 which demonstrate the flexion and extension movement of this joint with the flexion in the negative values and the extension in the positive values. Due to the equine morphology, it is not possible for this joint to achieve the positive values as shown in figure 24 and 25.

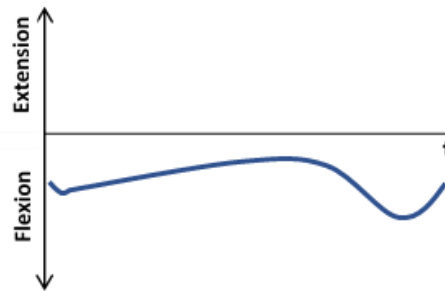


Figure 25 – Graphic of the sagittal plane’s movement of the joint n°8 which shows the flexion/extension movement of this joint.

Joint #9

The joint number 9 can be found in distal portion of the forelimbs and is anatomical designate as stifle joint. This joint join three bones: the femur, patella, and tibia, and three smaller joint: the femoropatellar joint, medial femorotibial joint and lateral femorotibial joint.

In the present study the joint n° 9 has two segments –tibia and fibula and femur with 3 markers in each segment as showed in table 13.

Table 13 – Description of the segments and markers of the joint number 9.

Joint Number	Related Segments	Segments Markers (Localization and acronym)
--------------	------------------	--

9	Tibia and Fibula	Tibial Tuberosity - PTIB Middle distance between marker PTIB and LTIB - MdTIB Proximal to the lateral malleolus of the Fibula - LTIB 2cm proximal to the medial malleolus of the Tibia - MTIB
	Femur	Greater trochanter of the femur - PFEM Middle distance between marker PFEM and DFEM - MdFEM Lateral Epicondyle of the Femur - DFEM

The figure 26 demonstrate the movement of the joint nº 9 in the standing position and in slight flexion position with the vector of the Z axis of each segment (orange arrows). In this joint the standing position (figure 26a) gives us a positive initial number of the angle of this joint and in a flexion position (figure 26b) that angle keeps positive during all the movement.

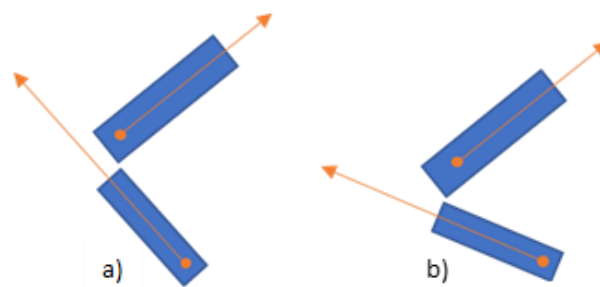


Figure 26 – Vectors of Z axis of each segment in the joint nº 9.

a) standing position; b) slight flexion position

In the figure 27 it is shown a graphic of the sagittal plane's movement of the joint nº9 which demonstrate the flexion and extension movement of this joint with the flexion in the positive values and the extension in the negative values. Due to the equine morphology, it is not possible for this joint to achieve the negative values as shown in figure 26 and 27.

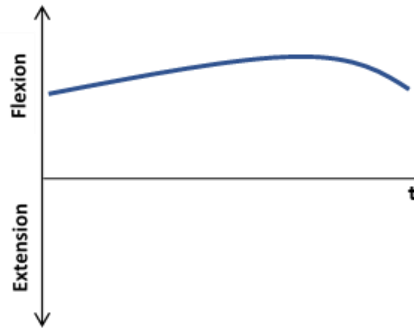


Figure 27 – Graphic of the sagittal plane’s movement of the joint n°8 which shows the flexion/extension movement of this joint.

Joint #10

The joint number 10 can be found in hindlimbs and is anatomical designate as coxofemoral joint also known as hip joint. This joint is formed by the proximal articular surface of the femur and the acetabulum of the pelvis.

In the present study the joint n° 10 has two segments – femur and pelvis with 3 markers in the first segment and 2 markers in the second segment as showed in table 14.

Table 14 – Description of the segments and markers of the joint number 10.

Joint Number	Related Segments	Segments Markers (Localization and acronym)
10	Femur	Greater trochanter of the femur - PFEM Middle distance between marker PFEM and DFEM - MdFEM Lateral Epicondyle of the Femur - DFEM
	Pelvis	Caudoventral Extremity of the coxal tuber – COXAL Ischial tuber - ISCHIAL

8.Example of 3D kinematic data vs. time of a set of trials

Interpretation of the data can be study by a brief definition encompass two concepts of the horse locomotion: The first concept is related with the pace during the forward progression. The second concept is related with the pattern of the limbs motion.

The examples show below are data from a horse with 12 years old that is a mixed breed horse, used in jumping competitions. From the data acquisition were chosen the first set of 10 trials, on each one with 2 steps without gaps in the acquisition software The trials are performed in the same day and the registration is in accordance with the validation of "no gaps" (no missing coordinates of all reflective markers placed on the horse) on the output of Nexus software⁴. Also the veterinary specialist decided that by visualization the walk is have a normal pattern.

8.1. *The pace*

The "pace concept" measure the pattern of the pace for walk, trot and gallop have different organizations and the interpretation work with the variability of the spatiotemporal parameters such as time and stride length, divided on support phase and swing phase. However, locomotion general speed are very dependent of the "walking by hand" characteristics. One can speculate about that looking for the next results. The "AKU" horse was very regular on the walk pace as show on the below table. It is "necessary" to approximate the time to two decimal places to find the justification for the coefficient of variation values. Therefore, these values of the horse's walking pace may be very dependent on the "handled walking and trotting kinematics " characteristics. But in other hand one can assume that the distribution of the step time pattern ("support time percentage") is dependent of the horse way of pace neuromusculoskeletal control even when a certain rhythm is "imposed" on him by external actions, be it the handled walking or the dressage training or competition.

⁴ Technical handbook Vicon Nexus 2.9 (<https://docs.vicon.com/display/Nexus210/Vicon+Nexus+User+Guide>)

HORSE : AKU steps "n = 20"									
Front LEFT					Front Right				
	step "time"	support "time percentage"	support "time"	swing "time"		step "time"	support "time percentage"	support "time"	swing "time"
average	1,46	67,23	0,98	0,48	average	1,46	67,30	0,98	0,48
desv pad	0,06	1,26	0,05	0,02	desv pad	0,06	0,95	0,04	0,02
coef var	4,04	1,87	4,98	4,60	coef var	4,07	1,41	4,57	4,43
max	1,59	70,00	1,09	0,52	max	1,57	68,71	1,06	0,51
min	1,35	63,89	0,89	0,44	min	1,35	65,52	0,89	0,43
mode	1,41	68,09	0,96	0,48	mode	1,48	67,57	1,00	0,50
Back LEFT					Back Right				
average	1,48	67,77	1,00	0,48	average	1,48	65,69	0,97	0,51
desv pad	0,06	1,10	0,05	0,02	desv pad	0,04	1,13	0,03	0,02
coef var	3,74	1,62	4,72	3,76	coef var	2,89	1,71	3,23	4,57
max	1,61	70,86	1,11	0,50	max	1,58	68,03	1,05	0,55
min	1,39	66,19	0,92	0,44	min	1,40	63,51	0,93	0,47
mode	1,51	68,42	1,04	0,46	mode	1,43	65,07	0,96	0,51

8.2. The angular kinematic pattern


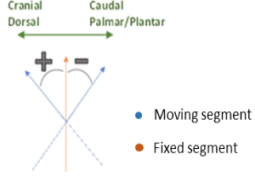
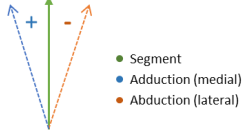
The second concept is related with the pattern of the limbs motion that organize the manner of inter segmental angular progression in accordance with the pace in the support phase and on the swing phase of each single limb and the correspondent temporal synchronization with the other ones.

Constantly dependent on the neuromusculoskeletal control is the development of the inter segmental angular velocities due the influence of those velocities on the mechanical energy transfer. A basic biomechanical concept demonstrate that the mechanical energy flows from the "fixed" mechanical segment to the "free" one. In support phase the mechanical energy flows from the upper segment to the support segment, in the swing phase it happens the opposite. The cited mechanical energy it depends from morphological components combine with the intersegmental angular velocity. The morphological (segment length and inertia) do not change but the self-control angular velocity will be determinant to understand the flow and quantification of mechanical energy.

In both concepts the variability is present from stride to stride as result of a normal motor behaviour defined as non-deterministic, therefore, standardised but not robotic. For the first concept the pace during the forward progression is study by descriptive statistics. For the second one, the adequate and more simplified solution is to study the behaviour variability, first isolating each stride from a homogeneous set of the same locomotion type (walk, trot, etc.) and form a wave that represents one stride behaviour; second checking the coefficient of variation of the set of waves found. The proposed process is the application of the wave-coefficient of variation seen before(Winter, 2009).

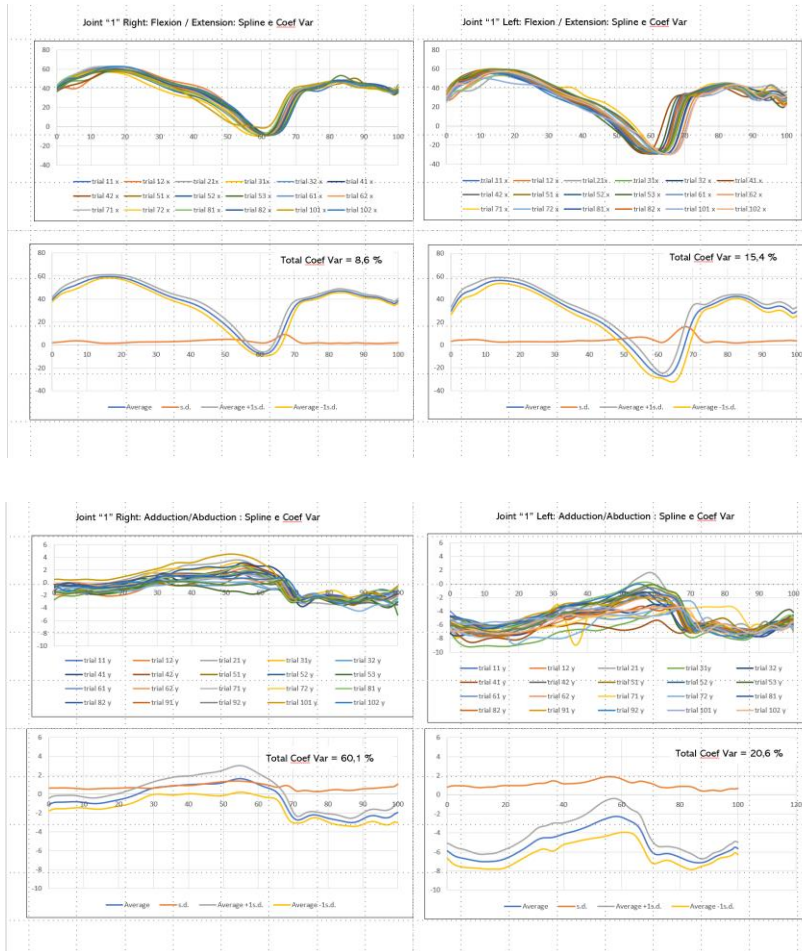
Angular of joint # 1 (support methodology in the previous pages)

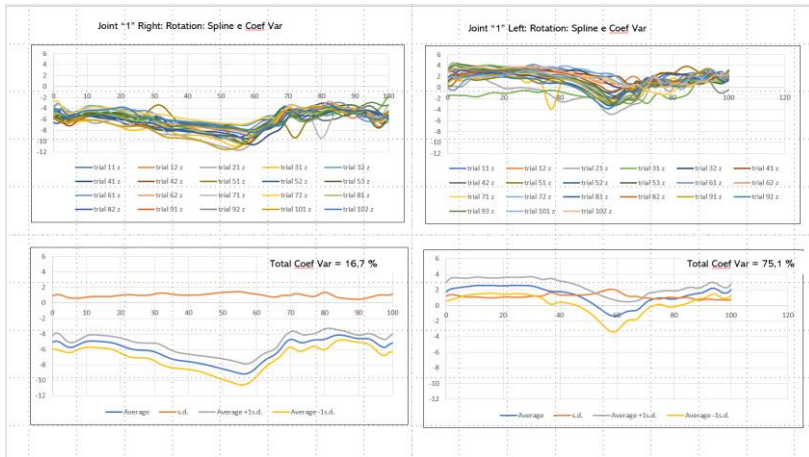
	Plane of rotation [Rules of analysis in the report]		
	Flexion /Extension	Adduction/Abduction	Rotation

	<p>Dot product of the longitudinal vectors, the Z axis of each segment.</p> 	<p>Dot product of the cranio/caudal vectors, the X axis of each segment</p> 	<p>Dot product of the cranio/caudal vectors, the Y axis of each segment.</p>
<p>[Nexus csv output data column]</p>	<p>[x]</p>	<p>[y]</p>	<p>[z]</p>

Our laboratory developed the software for compute the "spline" (normalization of "time" to 100%) and the "average" the "average plus and minus 1 standard deviation" and the "total coefficient of variation" of the behavior of each joint angle component.

Example of Joint#1. The sample is the same of the above: 20 steps of 10 trials without gaps:





BIBLIOGRAPHY OF REFERENCE

The literature searched was based essentially on the databases: PubMed, ScienceDirect

- Arkell, M., Archer, R.M., Guitian, F.J. and May, S.A. (2006) Evidence of bias affecting the interpretation of the results of local anaesthetic nerve blocks when assessing lameness in horses. *Vet. Rec.* 159(11):346-9. doi: <https://doi.org/10.1136/vr.159.11.346>
- Back, W., Bogert, A.J. van Weeren, P.R. van. Bruin, G. and Barneveld, A. (1993) Quantification of the locomotion of Dutch Warmblood foals. *Acta Anat (Basel)* 146(2-3):141-7. doi: <https://doi.org/10.1136/vr.159.11.346>
- Barrey, E. (1999). Methods, applications and limitations of gait analysis in horses. *Veterinary journal*, 157 1, 7-22. <https://doi.org/10.1053/tvj.1998.0297>
- Bragança, F., Rhodin, M., Wiestner, T., Hernlund, E., Pfau, T., van Weeren, P., Weishaupt, M. (2018) Quantification of the effect of instrumentation error in objective gait assessment in the horse on hindlimb symmetry parameters. *Equine Veterinary Journal*, 0 (3) 370-376 <https://doi.org/10.1111/evj.12766>
- Bragança, F., Hernlund, E., Thomsen, M., Waldern, N., Rhodin, M., Byström, A., van Weeren, R. Michael A. Weishaupt (2021) Adaptation strategies of horses with induced forelimb lameness walking on a treadmill. 53 (3) 600-611. <https://doi.org/10.1111/evj.13344>
- Brown, S., Stubbs, N., Kaiser, L., Lavagnino, M., Clayton H. (2015) Swing phase kinematics of horses trotting over poles. *Equine veterinary Journal*, v.47(1):107-112. doi: <https://doi.org/10.1111/evj.12253>
- Byström, A., Clayton, H., Hernlund, E., Rhodin, M., Egenvall, A. (2019) Equestrian and biomechanical perspectives on laterality in the horse *Comparative Exercise Physiology*: 16 (1)- Pages: 35 - 45 <https://doi.org/10.3920/CEP190022>
- Byström, A., Egenvall, A., Roepstorff, L., Rhodin, M., Bragança, F., Hernlund, E., van Weeren, R., Weishaupt, M., Clayton, H. (2018) Biomechanical findings in horses showing asymmetrical vertical excursions of the withers at walk. *PLoS ONE* 13(9): e0204548. <https://doi.org/10.1371/journal.pone.0204548>
- Chateau, H., Robin, D., Falala, S., Pourcelot, P., Valette, J., Ravary, B., & Denoix, J. M. (2009). Effects of a synthetic all-weather waxed track versus a crushed sand track on 3D acceleration of the front hoof in three horses trotting at high speed. *Equine Vet J.*, 41, 247–251. <http://doi.org/10.2746/042516409X394463>
- Clayton, H., Schamhardt, H., Willemen M., Lanovaz, J., Colborne, G. (1994) Comparison of the stride kinematics of the collected, working, medium and extended trot in horses *Equine veterinary Journal*, v.26 (3) 230-234. <https://doi.org/10.1111/j.2042-3306.1994.tb04375.x>

- Clayton, H. (2000) Kinematics and ground reaction forces in horses with superficial digital flexor tendinitis. *American journal of veterinary research*. 61 (2), 191-196. DOI: <http://doi.org/10.2460/ajvr.2000.61.191>
- Clayton, H., Sha, D., Stick, J. A., & Mullineaux, D. R. (2004). Three-dimensional carpal kinematics of trotting horses. *Equine Vet J.*, 36(8), 671–676. <http://doi.org/10.2746/0425164044848037>
- Clayton, H., Sha, D., Stick, J. A., & Elvin, N. (2007). 3D kinematics of the equine metacarpophalangeal joint at walk and trot. *Veterinary and Comparative Orthopaedics and Traumatology*, 20(2), 86–91. <http://doi.org/10.1160/VCOT-07-01-0011>
- Degueurce, C., Dietrich, G., Pourcelot, P., Denoix, J. M., & Geiger, D. (1996). Three-dimensional kinematic technique for evaluation of horse locomotion in outdoor conditions. *Medical and Biological Engineering and Computing*, 34(3), 249–252. <http://doi.org/10.1007/BF02520082>
- Ericson, C., Stenfeldt, P., Hardeman, A., Jacobson, I. (2000) The Effect of Kinesiotape on Flexion-Extension of the Thoracolumbar Back in Horses at Trot. *Animals* 2020, 10(2), 301; <https://doi.org/10.3390/ani10020301>
- Faber, M., Schamhardt, H. C., Van Weeren, P. R., & Barneveld, A. (2001). Methodology and validity of assessing kinematics of the thoracolumbar vertebral column in horses on the basis of skin-fixed markers. *American Journal of Veterinary Research*, 62(3), 301–306. <http://doi.org/10.2460/ajvr.2001.62.301>
- Fredricson, I., Drevemo, S., Dalin, G., Hjertén, G., & Bjorne, K. (1980). The application of high-speed cinematography for the quantitative analysis of equine locomotion. *Equine Veterinary Journal*, 12(2), 54–59. <http://doi.org/10.1111/j.2042-3306.1980.tb02309.x>
- Fuller, C.J., Bladon, B.M., Driver, A.J. and Barr, A.R.S. (2006) The intra- and inter-assessor reliability of measurement of functional outcome by c scoring in horses. *Vet. J.* 171, 281-286. <http://doi.org/10.1016/j.tvjl.2004.10.012>
- Hardeman, A., Byström L., Swagemakers, P., van Weeren, P. , Bragança F. (2000) Range of motion and between-measurement variation of spinal kinematics in sound horses at trot on the straight line and on the lunge *PLoS One*. 2020; 15(2): e0222822. <https://doi.org/10.1371/journal.pone.0222822>
- Hobbs, S., Bertram, J. Clayton, H. (2016) An exploration of the influence of diagonal dissociation and moderate changes in speed on locomotor parameters in trotting horses. June 2016 *PeerJ* 4(3):e2190. <http://doi.org/10.7717/peerj.2190>
- Hodson, E., Clayton, H., Lanovaz, J. (2000) The forelimb in walking horses: 1. Kinematics and ground reaction forces *Equine Veterinary Journal*, 32 (4), 287-294. <http://doi.org/10.2746/04251640077032237>
- Geiger, S. M., Reich, E., Bottcher, P., Grund, S., & Hagen, J. (2018). Validation of biplane high-speed fluoroscopy combined with two different non-invasive tracking methodologies for measuring in vivo distal limb kinematics of the horse. *Equine Veterinary Journal*, 50(2), 261–269. <http://doi.org/10.1111/evj.12717>

Gmel, A., Haraldsdóttir, E., Bragança, F., Cruz, A., Neuditschko, M., Weishaupt, M. (2022) Determining Objective Parameters to Assess Gait Quality in Franches-Montagnes Horses for Ground Coverage and Over-Tracking - Part 1: At Walk.

<https://doi.org/10.1016/j.jevs.2022.104166>

Alvarez, G., Wennerstrand, J., Bobbert, M., Lamers, L., Johnston, C., Back, W., van Weeren, P. (2007) The effect of induced forelimb lameness on thoracolumbar kinematics during treadmill locomotion. *Equine veterinary Journal*, 39(3):197-201.

<https://doi.org/10.2746/042516407x173668>

Hewetson, M., Christley, R.M., Hunt, I.D. and Voute, L.C. (2006) Investigations of the reliability of observational gait analysis for the assessment of lameness in horses. *Vet. Rec.*158, 852-858.

<https://doi.org/10.1136/vr.158.25.852>

Hobbs, S., Levine, D., Richards, J., Clayton, H. M., Tate, J., & Walker, R. (2010). Motion analysis and its use in equine practice and research. *Wiener Tierärztliche Monatsschrift -Veterinary Medicine Austria*, 97(1), 55–64.

Douglas, J., Moore-Colyer, M. (2009) The relationship between range of motion of lumbosacral flexion-extension and canter velocity of horses on a treadmill. *Equine Veterinary Journal*,

41(3):301-3. <https://doi.org/10.2746/042516409X397271>

Keegan, K. (2007) Evidence-Based Lameness Detection and Quantification. *Veterinary Clinics of North America: Equine Practice*. 23 (2). 403-423. <https://doi.org/10.1016/j.cveq.2007.04.008>

Keegan, K.G., Wilson, D.A., Wilson, D.J., Smith, B., Gaughan, E.M., Pleasant, R.S., Lillich, J.D., Kramer, J., Howard, R.D., Bacon-Miller, C., Davis, E.G., May, K.A., Cheramie, H.S., Valentino, W.L. and van Harreveld, P.D. (1998) Evaluation of mild lameness in horses trotting on a treadmill by clinicians and interns or residents and correlation of their assessments with kinematic gait analysis. *Am. J. Vet. Res.*59, 1370-1377.

Langlois, B., Froidevaux, J., Lamarche, L., Legault, C., Legault, P., Tassencourt, L., & Théret, M. (1978). Analyse des liaisons entre la morphologie et l'aptitude au galop au trot et au saut d'obstacles chez le Cheval. *Annales de génétique et de sélection animale*, 10(3), 443–474.

<http://doi.org/10.1186/1297-9686-10-3-443>

Lanovaz, J. L., Khumsap, S., Clayton, H. M., Stick, J. A., & Brown, J. (2002). Three-dimensional kinematics of the tarsal joint at the trot. *Equine Veterinary Journal*, 34(34 S), 308–313.

<http://doi.org/10.1111/j.2042-3306.2002.tb05438.x>

Meershoek, L.S., Schamhardt, H.C., Roepstorff, L. And Johnston, C. (2001), Forelimb tendon loading during jump landings and the influence of fence height. *Equine Veterinary Journal*, 33:

6-10. <https://doi.org/10.1111/j.2042-3306.2001.tb05349.x>

Moorman, V., Reiser, R., McIlwraith, C., Kawcak, C. (2012) Validation of an equine inertial measurement unit system in clinically normal horses during walking and trotting. *Am J Vet Res.* 73(8):1160-70.

<https://doi.org/10.2460/ajvr.73.8.1160>.

- Morris, R. G., & Lawson, S. E. M. (2010). A review and evaluation of available gait analysis technologies, and their potential for the measurement of impact transmission. <http://doi.org/10.1142/S0219519416300039>
- Nauwelaerts, S., Aerts, P., Clayton, H. (2013) Spatio-temporal gait characteristics during transitions from trot to canter in horses. *Zoology*. 116 (4), 197-204 <https://doi.org/10.1016/j.zool.2013.03.003>
- M. Rhodin, E. Persson-Sjodin, A. Egenvall, F. M. Serra Bragança, T. Pfau, L. Roepstorff, M. A. Weishaupt, M. H. Thomsen, P. R. van Weeren, E. Hernlund (2018) Vertical movement symmetry of the withers in horses with induced forelimb and hindlimb lameness at trot. *Equine Veterinary Journal*, 50 (6) 818-824. <https://doi.org/10.1111/evj.12844>
- Roepstorff, C., Dittmann, M., Arpagaus, S., Bragança, F., Hardeman, A., Sjödin, E., Roepstorff, L., Gmel, A., Weishaupt, M. (2021) Reliable and clinically applicable gait event classification using upper body motion in walking and trotting horses. *Journal of Biomechanics*, 114(4) 110-146. <https://doi.org/10.1016/j.jbiomech.2020.110146>
- Seino K., Secord, T. Vig, M., Kyllonen, S., DeClue, A. (2019) Three-Dimensional Kinematic Motion Analysis of Shivers in Horses: A Pilot Study. *Journal Equine Veterinary Science*. 79:13-22. Epub 2019 Mar 21. PMID: 31405492. <https://doi.org/10.1016/j.jevs.2019.03.006>
- Simonato, S., Bernardina, G., Ferreira, L., Silvatti, A., Barcelos, K., Fonseca, B., (2021) 3D kinematic of the thoracolumbar spine in Mangalarga Marchador horses performing the marcha batida gait and being led by hand-A preliminary report. *PLoS One*. Jul 6;16(7):e0253697. PMID: 34228737; PMCID: PMC8259994. <https://doi.org/10.1371/journal.pone.0253697>
- Solé M, Santos R, Gómez MD, Galisteo AM, Valera M. (2013) Evaluation of conformation against traits associated with dressage ability in unriden Iberian horses at the trot. *Res Vet Sci*. 2013 Oct;95(2):660-6. Epub 2013 Jul 21. PMID: 23880096. <https://doi.org/10.1016/j.rvsc.2013.06.017>
- Tijssen, M., Hernlund, E., Rhodin, M., Bosch, S., Voskamp, J., Nielen, M., Bragança, F. (2020) Automatic detection of break-over phase onset in horses using hoof-mounted inertial measurement unit sensors. *PLoS One*. 29;15(5):e0233649. doi: 10.1371/journal.pone.0233649. Erratum in: *PLoS One*. 5(7):e0236181. PMID: 32469939; PMCID: PMC7259550. <https://doi.org/10.1371/journal.pone.0233649>
- Thorpe CT, Marlin DJ, Franklin SH, Colborne GR. (2009) Transverse and dorso-ventral changes in thoracic dimension during equine locomotion. *Vet J*. 2009 Mar;179(3):370-7. doi: 2007.10.014. Epub 2007 Dec 3. PMID: 18061496. <https://doi.org/10.1016/j.tvjl>
- Unt VE, Evans J, Reed SR, Pfau T, Weller R. (2010) Variation in frontal plane joint angles in horses. *Equine Vet J Suppl*. 2010 Nov;(38):444-50. <https://doi.org/10.1111/j.2042-3306.2010.00192.x>

Weishaupt MA, Waldern NM, Amport C, Ramseier LC, Wiestner T. (2013) Effects of shoeing on intra- and inter-limb coordination and movement consistency in Icelandic horses at walk, tölt and trot. *Vet J.* 2013 Dec;198 Suppl 1:e109-13. <https://doi.org/10.1016/j.tvjl.2013.09.043>

Wiggers N, Nauwelaerts SLP, Hobbs SJ, Bool S, Wolschrijn CF, Back W (2015) Functional Locomotor Consequences of Uneven Forefeet for Trot Symmetry in Individual Riding Horses. *PLoS ONE* 10(2): e0114836. <https://doi.org/10.1371/journal.pone.0114836>

Winter, D. (2009). *Biomechanics and Motor Control of Human Movement*(4th ed.). Hoboken, New Jersey: John Wiley & Sons, Inc.